uOttawa

L'Université canadienne
Canada's university

FACULTÉ DES ÉTUDES SUPÉRIEURES ET POSTOCTORALES

uOttawa

L'Université canadienne
Canada's university

FACULTY OF GRADUATE AND POSDOCTORAL STUDIES

Sarah Margaret Mercer
AUTEUR DE LA THÈSE / AUTHOR OF THESIS

M.A.Sc. (Chemical Engineering)
GRADE / DEGREE

Department of Chemical Engineering
FACULTÉ, ÉCOLE, DÉPARTEMENT / FACULTY, SCHOOL, DEPARTMENT

Heterogeneous Photocatalysis : Design and Experimental Characterization of a New Photocatalytic Reactor for Wastewater Treatment

TITRE DE LA THÈSE / TITLE OF THESIS

Dr. J. Zhang
DIRECTEUR (DIRECTRICE) DE LA THÈSE / THESIS SUPERVISOR

Dr. Z. Duvnjak
CO-DIRECTEUR (CO-DIRECTRICE) DE LA THÈSE / THESIS CO-SUPERVISOR

EXAMINATEURS (EXAMINATRICES) DE LA THÈSE / THESIS EXAMINERS

Dr. D. Taylor

Dr. A. Tremblay

Gary W. Slater
Le Doyen de la Faculté des études supérieures et postdoctorales / Dean of the Faculty of Graduate and Postdoctoral Studies

Heterogeneous Photocatalysis: Design and Experimental Characterization of a New Photocatalytic Reactor for Wastewater Treatment

by

Sarah M. Mercer

Thesis submitted to the
Faculty of Graduate and Postdoctoral Studies
In partial fulfillment of the requirements
For the M.A.Sc. degree in
Chemical Engineering

Department of Chemical Engineering
Faculty of Engineering
University of Ottawa

Your file Votre référence
ISBN: 978-0-494-25806-4
Our file Notre référence
ISBN: 978-0-494-25806-4

Abstract

The objective of this study is to promote photocatalytic wastewater treatment by proposing a reactor design that employs a catalyst-coated, rotating, corrugated drum to increase the surface area, induce agitation and promote reactant and photon transfer to the surface. Corrugation profiles with surface areas ranging from 405 cm^2 to 3650 cm^2 were considered — the addition of corrugations improved the phenol degradation rate by up to 200 %. Based on an analysis of rotational speed and initial pollutant concentration, the reaction was found to be limited by the kinetics at 20 ppm and 40 ppm, but limited by phenol transfer to the reaction sites at 5 ppm. Finally, Langmuir-Hinshelwood kinetics was applicable with an average phenol adsorption coefficient of 0.120 L/mg and an increasing overall reaction rate constant with surface area. Further studies are necessary for the industrial use of such a reactor design including treatment of wastewater with varying characteristics, reactor design scaling and the applicability of this design for solar-activated applications.

Résumé

L'objectif de cette étude est de promouvoir le traitement photocalytique d'eau contaminée en proposant un réacteur composé d'un cylindre ondulé, couvert de catalyseur, tournant dans un basin rempli d'eau contaminée. En augmentant la surface du cylindre de 405 cm^2 à 3650 cm^2 par l'addition d'ondulations sur le cylindre, le taux de dégradation du phénol augmente jusqu'à 200 %. D'après les données obtenues avec les diverses vitesses rotationnelles et les concentrations initiales, la réaction démontre un plateau cinétique avec des taux de concentration de 20 ppm et 40 ppm, mais pour une concentration de 5 ppm le taux de dégradation augmente par rapport à la vitesse en augmentant la quantité de phénol qui entre en contact avec la surface du catalyseur. Finalement, la cinétique Langmuir-Hinshelwood est applicable avec un coéfficient d'absorption moyen pour le phénol de 0.120 L/mg et une constante de taux de réaction global augmentant par rapport à la surface du catalyseur. Afin de passer à la commercialisation de cette technique, il faut étudier, entre autres, le traitement de solvant avec des caractéristiques variantes, l'augmentation de l'échelle du réacteur et l'application de ce produit pour des projets activés par les rayons solaires.

Acknowledgements

Throughout the hard times and the good times, there are many people who helped guide me through. Some on a professional basis while others on a personal basis. I want to thank you all. Whether you realize it or not, everything you do makes a difference.

I'd like to mention in particular the following people who played a major role in my academic success:

- To my supervisors, Dr. Jason Zhang and Dr. Zdravko Duvnjak, thank you for your uninhibited technical guidance and discussion throughout my graduate studies, and for your financial support. I would also like to acknowledge the financial support I received from the University of Ottawa and NSERC.
- To Louis Tremblay, Gérard Nina and Franco Ziroldo, thank you for helping me build my apparatus and keep it running. Your expertise was a great help.
- To my colleagues, Nick Chan, Michelle Cooper, Jeff Harvey and Aaron Price, your assistance has been invaluable to me. I hope I helped you as much as you helped me.
- To my mentors throughout my studies at the University of Ottawa, Dr. David McLean and Dr. David Taylor, thanks for everything. Your advice and guidance have always been appreciated and taken to heart.
- To my parents, brothers and sisters (-in-law), thanks for standing by me through thick and thin. You may be far away, but you are always close at heart.
- To my friends who are always there to remind me that I can get through anything, no matter how challenging or intimidating.

- To Marc Meunier, thanks for everything — I can't begin to put it all in words.

Without all of you, I could never have accomplished what I have, or at least it would not have been nearly as much fun!

This is just one leg of the journey - what I have taken from this experience will guide me through all the rest.

Contents

List of Tables

List of Figures

Chapter 1

Introduction

Photocatalysis is an environmentally-friendly purification technique for air, water and soil contaminated with persistent organic compounds, recalcitrant chemicals, bacteria and micro-organisms. Photodegradation is a desirable treatment because it requires only an oxide semiconductor catalyst (often TiO_2 which has low toxicity, low cost, high stability and high activity [33, p.157]) and a light source (often ultra-violet) to activate the photocatalyst. Furthermore, the photocatalyst can be reused, the ultra-violet light source can be replaced by solar, complete mineralization of many contaminants is achievable and the operating conditions are generally ambient. Therefore, photocatalytic contaminant degradation is the quintessential alternative for air, soil and water treatment.

However, some barriers exist that prevent the commercialization and widespread use of photocatalysis, such as a low-order dependency of reaction rate on light intensity, inefficiencies due competing recombination reactions and limitations in photon and reactant transfer to the catalyst surface. Overcoming these challenges is an essential step in ensuring that photodegradation becomes a prevailing technology for the treatment of polluted media.

The objective of this study is to promote photocatalytic wastewater treatment by proposing a photoreactor design that employs a catalyst-coated, rotating, corrugated drum to increase the catalyst surface area, induce agitation of the reaction medium and promote transfer of reactants and photons to the catalyst surface. Consequently, this design aims to advance photocatalytic contaminant removal by providing a reactor system that prevails over current commercialization barriers.

This thesis explores photocatalysis by beginning with a review of the available literature involving the mechanisms, kinetics, catalysts and contaminants of photocatalytic reactions; the reported effects of various reaction parameters such as temperature, dissolved oxygen, pH, rotation, UV transmission, catalyst surface area, initial contaminant concentration and hydrogen peroxide addition; the current and potential applications of photocatalytic reactions; and the reactor configurations that have been previously studied. Based on the literature survey, the photoreactor configuration that was implemented is presented. The materials and methods used for evaluation of the reactor design are also introduced such as the chemicals, reactor equipment, catalyst immobilization techniques, system start-up, experimental procedure and analysis methods. The results of the experimental runs are then presented including the reproducibility of the results; the effect of drum configuration, rotational speed, initial concentration and illumination profile; and further analysis to determine the presence of reaction intermediates and by-products and the applicability of Langmuir-Hinshelwood kinetics. Finally, the major conclusions and recommendations for future study are recounted.

Chapter 2

Literature Review

2.1 Photocatalysis

The purification of air, water and soil polluted with toxic recalcitrant chemicals and micro-organisms can be achieved via photodegradation using a semiconductor catalyst and an ultra-violet light source. This section explores the mechanism and kinetics behind photocatalytic reactions, the catalysts and contaminants commonly used in photocatalysis, the effects of various reaction parameters on photodegradation rates, some applications for photocatalysis and several previously reported photoreactor configurations.

2.1.1 Reaction Mechanism

Photocatalytic processes are generally enhancements or substitutions for the purification of air, soil, or water via high-temperature incineration, activated sludge digestion and other physicochemical treatments by providing environmentally-sound alternatives for the destruction of bacteria, viruses and other micro-organisms, cancer cell inactivation, control of odorous chemicals, water photosplitting, nitrogen fixation and oil spill cleaning

[29]. The key elements of photocatalytic reactions are: 1. the light source which can be either solar or ultra-violet lamps and can be immersed in the reaction medium, external to the reaction medium, or distributed to the reaction medium by an external source such as a reflector; 2. the catalyst, generally a semiconductor oxide, which can be immobilized on the reactor surface, or contained within the reaction medium; and 3. the contaminant which is typically an air or water medium with an organic compound pollutant. There are five main steps in photocatalytic reactions [28]:

1. Reactant transfer from the reaction medium to the catalyst surface
2. Reactant adsorption
3. Reaction
   (a) Photon absorption by the catalyst
   (b) Electron-hole pair creation
   (c) Electron transfer reactions
4. Product desorption
5. Product removal from the catalyst-medium interface

In the photocatalytic reaction (step 3), the semiconductor catalyst achieves molecular excitation by absorbing photons (hv) with the appropriate energy from the illumination source. One common catalyst, titanium dioxide (TiO_2), has a band gap energy (E_g) of 3.2 eV which corresponds to an illumination wavelength of approximately 400 nm. When the semiconductor is excited with wavelengths slightly shorter than the band gap (for TiO_2 in the range of 300 nm to 400 nm) the formation of electron-hole pairs occurs. Therefore, there exists a mobile excited electron in the high energy conduction band (cb) and an electron hole in the low energy valence band (vb), as shown in Equation 2.1.

$$TiO_2 + hv \rightarrow e^-_{cb} + h^+_{vb} \tag{2.1}$$

Once the electron-hole pairs are generated there are two competing options. Either they recombine which is one of the main problems affecting the photoefficiency of such reactions by consuming photon energy [53], or parallel oxidation and reduction reactions are initiated by the electron-hole and the mobile electron respectively. Once these reactions are initiated, the oxidation of organic compounds and reduction of dissolved metal ions occurs. This process is depicted in Figure 2.1.

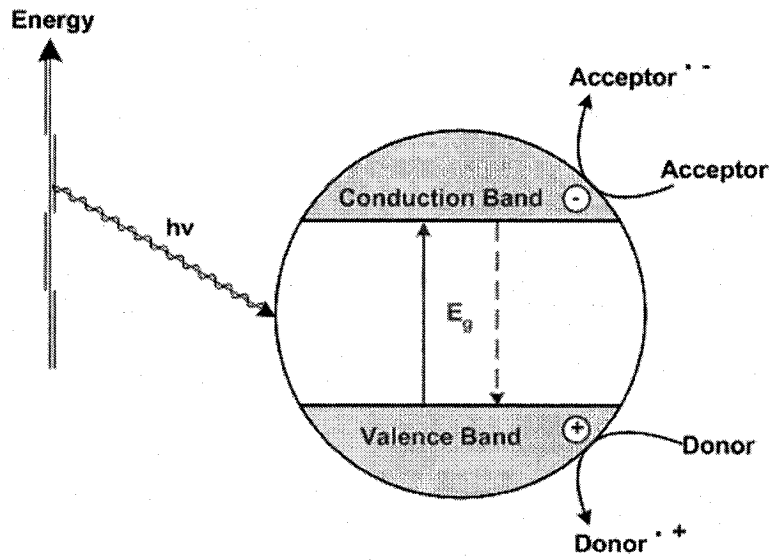

Figure 2.1: General photocatalytic reaction process [10]

Photocatalytic reactions use photons from the illumination source to provide desirable reaction sites on the catalyst surface and thus promote reactions to oxidize organic compounds leaving only carbon dioxide and water as the products. Therefore, photocatalysis provides environmentally-sound destruction of pollutants. Equation 2.2 shows the general stoichiometry for the photocatalytic degradation of organic compounds [29] — the specific stoichiometry for the complete destruction of a phenol pollutant is shown

in Figure 2.2.

$$C_xH_yX_z + \left(x + \frac{y-z}{4}\right) O_2 \xrightarrow{h\nu} xCO_2 + zH^+ + zX^- + \left(\frac{y-z}{2}\right) H_2O \qquad (2.2)$$

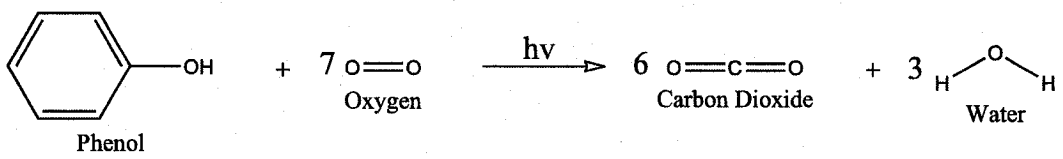

Figure 2.2: Photocatalytic reaction of phenol

Despite the desirable end-products of complete photocatalytic degradation, various reaction intermediates are formed and are not entirely degraded during the reaction. One aim of many photocatalytic degradation studies is to monitor the presence of these compounds and design reaction parameters that promote their degradation and thus reaction completion. Figure 2.3 shows the structures of commonly reported reaction intermediates for the photodegradation of phenol [25, 70, 81].

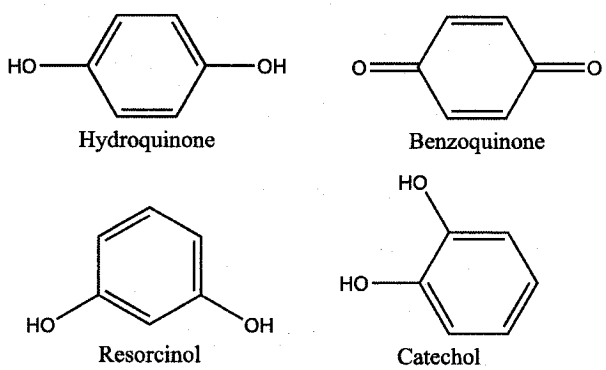

Figure 2.3: Reaction intermediates of phenol photodegradation

Sobczński et al. [70] executed a qualitative study on the intermediates of phenol photooxidation to elucidate the mechanism and kinetics of such reactions using an air lift loop slurry reactor. In this study, only trace amount of resorcinol were measured, so it is not considered a major contributor to the reaction intermediates. As shown in

Figure 2.4, after three hours there remained a 17 % discrepancy between the amount of reaction intermediates (hydroquinone-HQ, catechol and benzoquinone-BQ), total organic compounds (TOC) and phenol in the system. This indicates that other intermediates are present in the mixture that have not yet been reported.

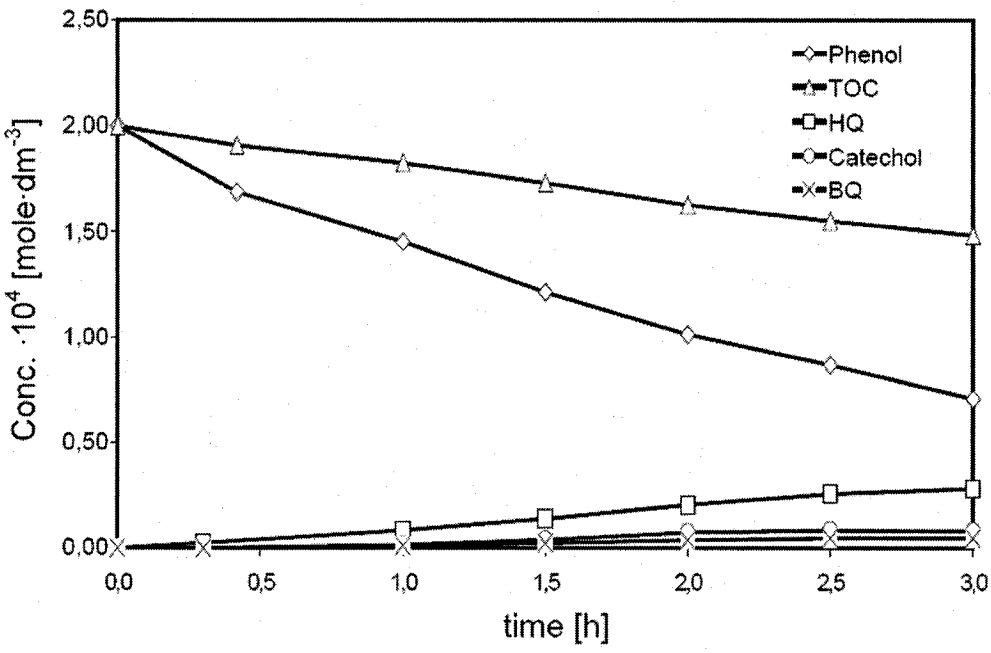

Figure 2.4: HPLC and TOC analysis results [70]

Based on the quantitative analysis of the reaction intermediates, Figure 2.5 shows a possible, but admittedly incomplete, mechanism for the photodegradation of phenol with a titanium dioxide catalyst [70].

2.1.2 Reaction Kinetics

Photocatalysis has been shown to follow Langmuir-Hinshelwood first-order kinetics to near complete pollutant degradation [3, 4, 15, 18, 24, 29, 37, 44, 70, 72, 76]. If the reactant and solvent are absorbed on the catalyst surface and do not compete for reaction sites, the Langmuir-Hinshelwood kinetics follows Equation 2.3, where: R is the reaction rate,

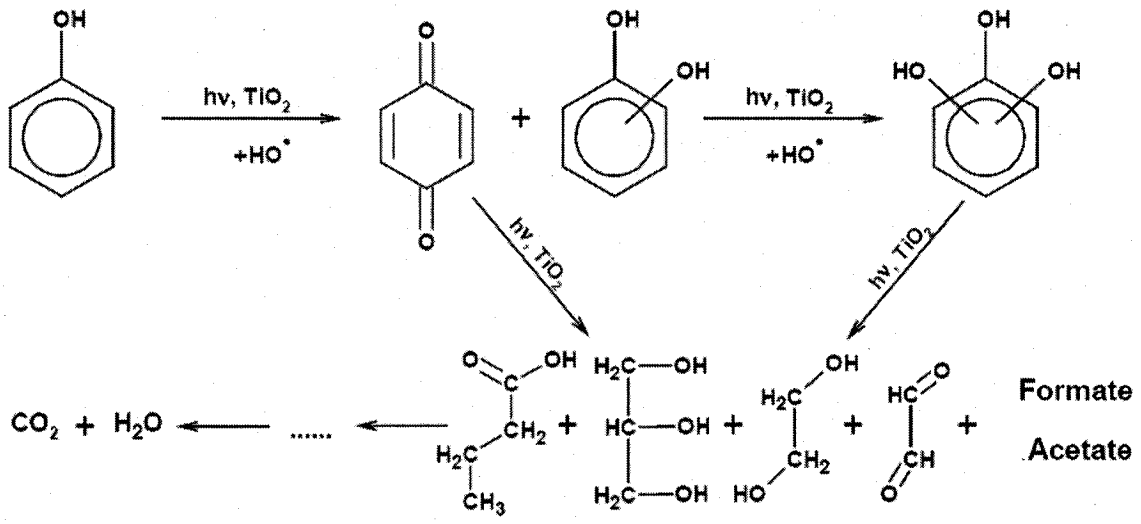

Figure 2.5: Potential phenol degradation mechanism [70]

C is the reactant concentration, t is time, k_r is the overall reaction rate constant and K is the adsorption coefficient of the reactant.

$$R = \frac{-dC}{dt} = \frac{k_r K C}{1 + KC} \tag{2.3}$$

Equation 2.3 can be rearranged to form Equation 2.4. Therefore, $1/R$ (or $1/(-dC/dt)$) can be plotted against $1/C$ to form a linear dependence where the slope is $1/(k_r K)$ and the y-intercept is $1/k_r$. The overall reaction rate constant and the adsorption coefficient of the reactant can be estimated from the slope and y-intercept of the linear trend for the experimental kinetic data.

$$\frac{1}{-dC/dt} = \frac{1}{k_r} + \frac{1}{k_r K}\left(\frac{1}{C}\right) \tag{2.4}$$

From these equations, it is evident that at low concentrations of the reactant, the reaction rate approaches $k_r KC$ and there is an apparent first-order reaction with a rate constant of $k_r K$. However, at high substrate concentrations the reaction rate approaches

a limiting value of k_r and a zero-order reaction occurs as the rate is independent of the substrate concentration. Therefore, in photocatalytic reaction kinetics a first-order reaction is primarily observed when the substrate concentration is high, then as the concentration decreases a transition zone occurs and finally when a sufficiently small concentration of reactant remains a zero-order reaction rate is observed.

These kinetics are shown in Figure 2.6 in terms of the degradation rate at varying concentrations. At low concentrations the degradation rate increases with increasing concentration (first order), but as the concentration increases the degradation eventually approaches an asymptotic rate where it ceases to increase regardless of further increasing concentrations (zero order).

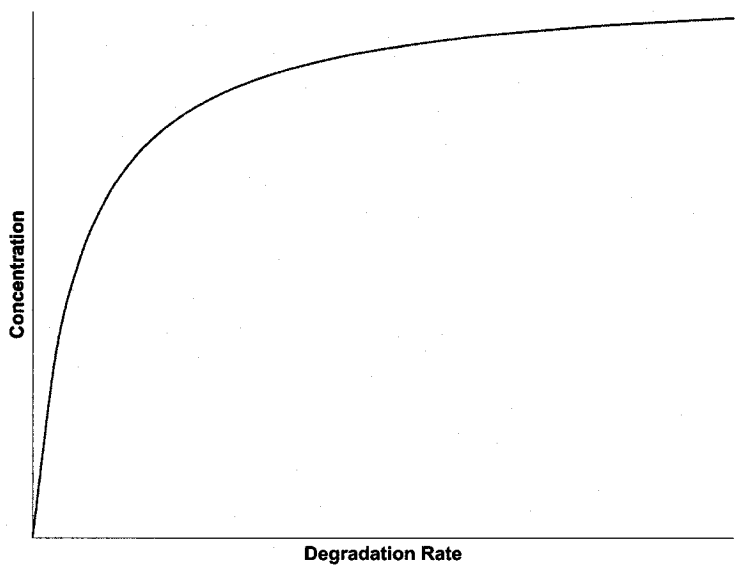

Figure 2.6: Langmuir-Hinshelwood kinetics

2.1.3 Catalysts and Contaminants

A photocatalyst is a material that has the ability to generate sites for photoreactions by absorbing light photons and is not consumed in the reaction. Semiconductors are

used as photocatalysts because they do not have continuous energy levels like metals; semiconductors possess the unique characteristic of void energy regions between the top of the valence band and the bottom of the conduction band known as the band gap. Therefore, as previously described, when electrons are photoexcited they jump from the filled valence band to the vacant conduction band thereby allowing sufficient time for the oxidation and reduction reactions to occur in the generated reaction sites. If the recombination of the mobile electron and the electron-hole occurs before the reactions proceed, significant energy is wasted and the photoefficiency of the process decreases dramatically.

Some characteristics of good semiconductor photocatalysts are: high photoactivity, high photostability, high resistance to photocorrosion, non-toxicity and chemical and biological stability. Although many semiconductors have been studied (including: SiO_2, TiO_2, ZnO, WO_3, CdS, ZnS, $SrTiO_3$, SnO_2, WSe_2, V_2O_5 and Fe_2O_3), TiO_2 is a widely accepted photocatalyst for environmental applications. Furthermore, in some cases such as the photooxidation of cyanide, titanium dioxide is the only catalyst that is photoactive enough to satisfactorily degrade the pollutant [47]. Titanium dioxide has sufficient energy in the electron-holes to oxidize organic compounds, good photooxidation kinetics and stability in aqueous and photoelectric environments [11]. Most types of organic and inorganic compounds can be degraded with a titanium dioxide photocatalyst; some categories of compounds that can be degraded are aliphatics, aromatics, surfactants, detergents, dyes, pesticides and herbicides [11]. In addition, heavy metals can been reduced via photocatalysis.

Phenol and phenol derivatives are often used as model pollutants [3, 4, 12, 18, 25, 32, 42, 43, 60, 69, 70, 81, 88]. Phenol is frequently found in the environment due to industrial and domestic activities because it is a common constituent of pesticides, herbicides,

pharmaceuticals and industrial discharge from plastics, resins, steels, dyes and organic chemical production [52, p.131]. In low concentrations, phenol can be found in foods, ointments and antiseptics; however, in large concentrations it may cause serious health risks such as heart, liver, kidney and lung diseases. The most common technique for phenol degradation is biological [14, 20, 22, 36, 48, 49, 50, 66, 68, 79, 82], but phenol degradation via chemical oxidation [54] has also been studied.

2.2 Reaction Parameters

Photocatalytic reactions are affected by various parameters such as temperature, dissolved oxygen content, pH, rotational speed (where applicable according to the reactor design), UV transmission, catalyst immobilization, initial contaminant concentration and hydrogen peroxide addition. This section reviews some of the literature regarding the effects of these parameters.

2.2.1 Temperature

Since the nature of photocatalytic reactions involves a temperature increase if it is not controlled, a study of the effect of temperature is an important part of photocatalytic characterization. Trillas et al. [74] studied the effect of reaction medium temperature on the contaminant degradation rate in a slurry TiO_2 reactor using phenoxyacetic acid as the model pollutant. Due to the rapid kinetics of the photocatalytic reaction, the effect of temperature on the reaction rate within the range of 25 °C to 76 °C was almost negligible. Similar results were found in a study by Yawalkar et al. [81] using a solar reactor with a TiO_2 catalyst and phenol as the model pollutant. In this case, the temperature was kept constant in one reactor at 38 °C and left uncontrolled in the other reactor where it

ranged from 38 °C to 75 °C. A comparison of these two reaction conditions showed very little effect of temperature on the degradation rate.

Other studies, however, show conflicting results. For example, Hofstadler et al. [30] found that the decomposition rate increased with temperature from 0.28 mg/Lh at 11.7 °C to 1.08 mg/Lh at 56.7 °C using a fused-silica glass fiber reactor with TiO_2 as the catalyst and 4-chlorophenol as the model pollutant. Andreozzi et al. [8] studied the effect of temperature on acidic and basic solutions in an immobilized TiO_2 annular reactor with 4-nitrophenol as the contaminant. A slightly negative effect on reaction rate with increasing temperature was found in the acidic solution (pH = 3) and a slightly positive effect was found with increasing temperature in the basic solution (pH = 8.5).

In general, a weak dependence of photodegradation rate on the reaction media temperature is reported; in addition, the decreased solubility of oxygen in the solution and the decreased concentration of mobile electron holes are undesirable side effects of temperature increase [11]. Since photocatalytic degradation rates are not strongly dependent on temperature, the temperature-limiting steps are not the rate-limiting steps [24].

2.2.2 Dissolved Oxygen

As shown in Equation 2.2 and Figure 2.2, oxygen is an important reactant in the conversion of organic species to carbon dioxide and water via photocatalytic degradation. Matthews and McEvoy [44] studied the effect of various reaction parameters on the degradation of phenol in an annular reactor with TiO_2 as the catalyst. They reported that the photodegradation rate increases when the dissolved oxygen concentration increases.

In a more recent study of 3,4-dichlorophenol photodegradation, Axelson and Dunne [9] confirmed the results found by Matthews and McEvoy and also showed that retarding the competing electron-hole recombination step is not the primary cause of the degradation

rate enhancement demonstrated by oxygen addition. Instead, the dissolved oxygen acts as a hydrogen atom acceptor in the hydroxyl addition to the phenyl ring and an electron transfer inhibitor at defective titanium sites. Therefore, dissolved oxygen is an essential component of organic compound photocatalytic degradation.

2.2.3 pH

The literature results regarding the effect of pH on photodegradation rates are inconclusive. Some studies have shown slightly increasing photodegradation rates of phenols with increasing pH values. For example, Abdullah et al. [1] observed maximum oxidation rates at pH values greater than 3.4 although the dependence was marginal; Matthews and McEvoy [45] studied a pH range of 3.5 to 8.5 and found a marginal increase in degradation rate with increasing pH; Ku and Hsieh [37] and Trillas et al. [75] also found the same marginal effect between pH values of 3 and 11; and Tanaka and Saha [71] confirmed this phenomena with alkaline solutions having higher degradation rates than acidic solutions.

In a study of immobilized titania on optical fibres, Hofstadler et al. [30] found that the degradation rate of 4-chlorophenol actually decreased with increasing pH from 3 to 5.8; however, this is inconsistent with most other literature data. In addition, other studies found that there was no significant effect of pH on phenol degradation rates, but higher concentrations of reaction intermediates were found at higher pH values [8, 72].

Despite the conflicting results of the effect of pH on photodegradation rate, a weak dependence of the rate on the pH is expected (less than one order of magnitude for the entire pH range) because of a change in surface charge and ionization state of the photocatalyst and thus its adsorption capabilities [11, 24]. In addition, a study of phenol photodegradation using a titania slurry catalyst and solar radiation demonstrates an

optimal pH value of 6 which is the isoelectric point of titanium dioxide [38].

2.2.4 Rotation

Although many photoreactor designs are not capable of rotation, the benefits of rotation and the effects of rotational speed for certain reactor configurations are reported in the literature. For example, studies by Sczechowski et al. [61, 62] use a light-dark cycling technique to enhance the photoefficiency by 500 % with an optimal illumination period of 72 ms and dark recovery time of 1.45 s. The dark period is significantly longer than the light period because the dark phase promotes the oxidation of organic compounds and thereby decreases the amount of reaction intermediates in the system and the occurrence of undesirable side reactions.

A study by Zhang et al. [83] promotes rotating photoreactors by completing studies with a platinum-loaded TiO_2 catalyst on a rotating drum photoreactor to degrade phenol. They determined that the photodegradation rate is controlled by the mass transfer of the pollutant to the illuminated surface until the critical rotational speed is reached and then the rate is controlled by the kinetics of the degradation reaction. Therefore, the degradation rate increases with increasing rotational speed until the critical rotational speed is reached (25 rpm) and once this speed is reached the degradation rate remains constant.

A study of rotational speed effects by Hamill et al. [27] shows a step-wise increase in degradation rate with rotational speed using a photoreactor system incorporating four rotating discs. In the range of speeds tested, three regions were observed: $0 - 20$ rpm (k_r @ 5 rpm $= 0.0128$ min^{-1}), $20 - 90$ rpm (k_r @ 67 rpm $= 0.0177$ min^{-1}) and > 90 rpm (k_r @ 136 rpm $= 0.0136$ min^{-1}). These steps are due to changing mass transfer properties of the reactor system. Although this is inconsistent with the results provided by Zhang et

al. [83], the study by Hamill et al. was completed over a much larger range of rotational speeds and is thus more comprehensive.

2.2.5 UV Transmission

Since ultra-violet light provides the photons necessary for the electrons to jump from the conduction band to the valence band, the intensity of the light is an important parameter in photocatalytic reactions. The energy of the photons is inversely proportional to the wavelength of the light and the energy input of the process is based primarily on the intensity of the incident light. In a study of the effect of light wavelength using an annular photocatalytic reactor with phenol as the model pollutant, Matthews and McEvoy [44] found that shorter wavelengths (254 nm) promoted higher degradation rates than longer wavelengths (350 nm). This was confirmed by Hofstadler et al. [44] in a study of 4-chlorophenol degradation; they also found that a smaller amount of intermediates were formed at shorter wavelengths because of the greater photon energy associated with those wavelengths.

In a study of solar-assisted photodegradation [81], experiments using a reflector to concentrate the light had five times higher degradation rates than those without the reflector and the rate was found to be proportional to the square root of the intensity. Increasing degradation rates with increasing light intensities has been shown in other literature as well [42, 59], and it was reported by Ollis et al. [51] via Equations 2.5, 2.6 and 2.7 where I is the intensity of the light and k_r is the degradation rate.

$$When\ I\ is\ low: \ k_r \propto I^{1.0} \tag{2.5}$$

$$When\ I\ is\ medium: \ k_r \propto I^{0.5} \tag{2.6}$$

$$When\ I\ is\ high: \ k_r \propto I^{0.0} \tag{2.7}$$

2.2.6 Catalyst Surface Area

The nature of the catalyst in photocatalytic processes is crucial to the performance of the system. Studies indicate that increasing the surface area of the catalyst particles or the loading of the catalyst significantly enhances the degradation rate [11, 81]. This is due to a greater production of reaction sites for the photodegradation to occur. In addition, when optimizing the degradation rate based on the incident light wavelength, Matthews and McEvoy [44] found that the optimal degradation rate which occurred at the lower wavelength actually required less catalyst loading than was necessary at the higher wavelength. Furthermore, it has been found in a study of the degradation of 2,4-dichlorophenol with TiO_2 slurries that increasing the catalyst loading increases the removal rate to a limiting value at 1.4 g/L of TiO_2; increasing the catalyst loading beyond this limiting value decreases the degradation rate [37]. This is said to be due to the inhibited light penetration that accompanies the increased catalyst loading. In agreement with this study, Crittenden et al. [16] found that increasing the light intensity increases the optimal catalyst loading because with increased light intensity the light has an enhanced ability to penetrate the catalyst.

There have been various studies optimizing the photodegradation rate based on immobilized TiO_2 catalysts on corrugated plate reactors [65, 85, 87, 88]. These studies show that corrugated-plate photoreactors have significantly faster pollutant conversion

(up to 150 %), are more energy efficient and have higher mass transfer rates (up to 600 %) than flat-plate reactors. This performance improvement is due to the unique ability of the corrugation profile to deliver reactants to the illuminated catalyst surface area and to recapture reflected light. The corrugations also provide an increased surface area for catalyst immobilization and thus increase the amount of available reaction sites. Furthermore, it was also determined that the angle of the corrugations on the reactor plate is an important performance factor because decreasing the corrugation angle not only increases the surface area, but also increases the photon delivery to the catalyst surface and increases the ability of the reactor to recapture and use reflected light rays [85].

2.2.7 Initial Concentration

Some studies have shown that the photodegradation rate of phenol is independent of the initial concentration of the substrate in the reaction medium. For example, in a study of solar-assisted photodegradation with initial phenol concentrations between 71 ppm and 480 ppm [81], no dependency of degradation rate on concentration was found.

Other studies using lower initial concentrations of substrate show a dependence of reaction rate on initial concentration. For example, phenol degradation in an air lift loop reactor with initial pollutant concentrations between 4.7 ppm and 18.8 ppm [70], demonstrated a scattered, but linear dependence between the initial concentration and the degradation rate. Another study confirmed these results at very low phenol concentrations using immobilized TiO_2 on a glass reactor tube [42]. In addition, a study of solar radiation in a TiO_2 slurry reactor showed an optimal initial phenol concentration of 30 ppm [38]. A study of a large scale multiple tube reactor [59] also showed an increasing reaction rate with increasing initial concentration from 1 ppm to 50 ppm.

With an annular photocatalytic reactor [45, 44], it was found that the degradation rate of phenol increased with increasing concentration, but at low concentrations the effect was much stronger than that at higher concentrations. Therefore, it has been demonstrated that there is a dependence of photodegradation rate on the initial substrate concentration for the degradation of phenol at low concentrations (less than 50 ppm), but at high concentrations (greater than 50 ppm) there is negligible dependence. This phenomenon is consistent with the Langmuir-Hinshelwood reaction kinetics previously discussed.

2.2.8 Hydrogen Peroxide

Similar to photocatalytic degradation, organic compounds can be completely degraded using hydrogen peroxide according to the reaction in Equation 2.8.

$$C_6H_5OH + 14H_2O_2 \rightarrow 6CO_2 + 17H_2O \tag{2.8}$$

The addition of hydrogen peroxide to photocatalytic reactions enhances the degradation rate because it removes surface trapped electrons and thus lowers the electron-hole recombination rate, it photolytically splits to produce hydroxyl radicals and it supplies oxygen to the system [51]. In a comparison of solar photocatalytic and photochemical degradation [81], the phenol degradation rate in the photochemical process was slightly faster than in the photocatalytic process, but there were higher concentrations of reaction intermediates in the photochemical process and the total organic compound degradation rate was the same in both cases. Therefore, a comparison of the expected operational costs for a reactor with a 1 m^3/h effluent flow capacity and 200 mg/L initial phenol concentration (photocatalytic 0.4 $/h and photochemical 1.8 $/h) showed that the photocatalytic process has the potential to be a more viable option.

Photocatalytic reaction rates are known to be enhanced when low concentrations of hydrogen peroxide are present because it accepts conduction band electrons and therefore augments the charge separation [26, p.7] [30]. However, the instability and corrosiveness of concentrated hydrogen peroxide limit its applicability for photocatalytic reactions despite enhancing the degradation rate [42].

2.3 Applications

There have been several review articles published that indicate the current and potential applications of photocatalytic reactions [2, 4, 10, 28, 29, 53]. For example, TiO_2 has been used as a coating to create self-cleaning surfaces that degrade oily and organic deposits; a purification and deodorization technique for indoor, outdoor and effluent air; a water purification technology to produce drinking water from various sources, to clean wastewater and to remediate contaminated groundwater; a water-splitting procedure; a method for cooling buildings via catalyst coatings and smart windows; and a medical technique for cancer treatment via organic matter degradation and for self-sterilizing and self-cleaning catheters [2]. In addition, slurry TiO_2 photoreactors have been shown to be successful in degrading organic coloured compounds that exist in wastewater from the textile dyeing industry so that those waters can be reused within the industry [39, 40]. Photocatalytic reactions are also useful for cleaning waters that have been contaminated with pesticides and herbicides so that they can be reused [2, 73].

On the basis of wastewater treatment, photocatalysis is useful for degrading organic and inorganic pollutants and recovering noble metals. Some of the organic pollutants that have been studied and deemed successfully degraded via photocatalysis are alkanes, haloalkanes, aliphatic alcohols, aliphatic carboxylic acids, alkenes, haloalkenes, aromatics, haloaromatics, nitrohaloaromatics, phenolic compounds, halophenols, amides, aro-

matic carboxylic acids, acids, surfactants, herbicides/pesticides, organo-phosphorus and dyes [11, 28].

Despite the potential for photocatalysis in air, water and soil purification technologies, there are few commercial or industrial applications [10]. Some of the barriers that prevent photocatalytic reactions from full-scale commercialization and acceptance are cost and photoefficiency [10, 53]. Thus, solar applications are quite promising and studies are necessary to overcome the low-order dependency of photocatalysis on light intensity and to prevent electron-hole recombination reactions. Although immobilized catalyst configurations have lower surface area to volume ratios in comparison to slurry reactors and have inefficiencies due to light scattering and absorption by the reaction medium, they are promising for commercial applications because it is not necessary to remove the catalyst from the reaction medium via filtration, centrifugation, or coagulation/flocculation [29]. Despite the drawbacks of photocatalytic degradation, some reactor configurations are used for actual and pilot plant water treatment systems such as parabolic trough, thin film fixed bed, compound parabolic collecting, double skin sheet and fluidized bed [10].

Deutsche Bundesstiftung Umwelt (DBU) in Osnabruck, Germany has developed a highly efficient photocatalytic reactor for the degradation of pollutants that are resistant to biological degradation. They use a titania catalyst immobilized on glass tubes. Figure 2.7 shows the laboratory scale reactor that is used to validate the titanium dioxide coating and Figure 2.8 shows the pilot scale photocatalytic reactor that is used by DELTA Umwelt-Technik GmbH in Teltow, Germany to decontaminate groundwater by photocatalysis and air stripping [31]. These reactors are low maintenance and, although they are not currently operated with solar radiation, they can be easily adapted for this use.

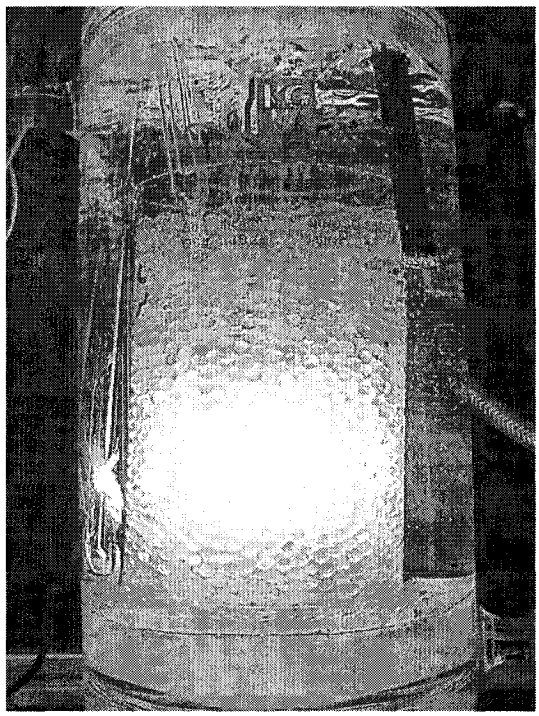

Figure 2.7: DBU laboratory scale photocatalytic reactor [31]

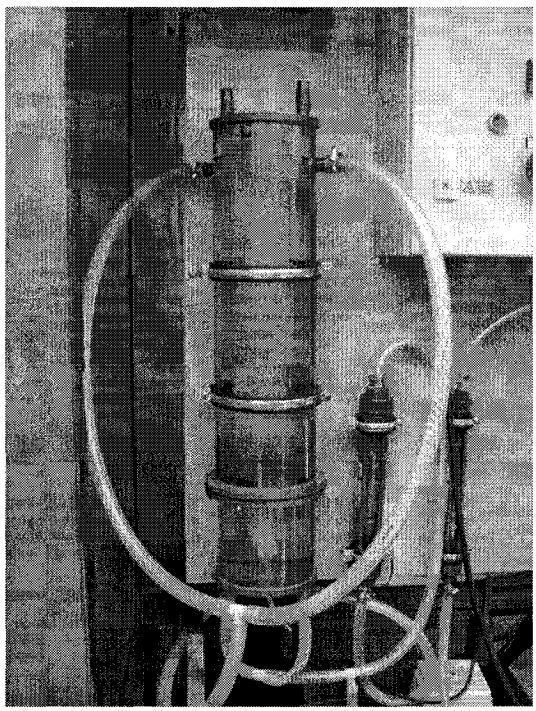

Figure 2.8: DBU pilot scale photocatalytic reactor [31]

In addition, Purifics Environmental Technologies Inc. [57] in London (Ontario, Canada) has developed a photocatalytic water treatment system called Photo-Cat® that can be used for groundwater remediation and industrial wastewater treatment (Figure 2.9). They use a suspended titania catalyst system that incorporates a filtration process to remove the catalyst from the reaction medium.

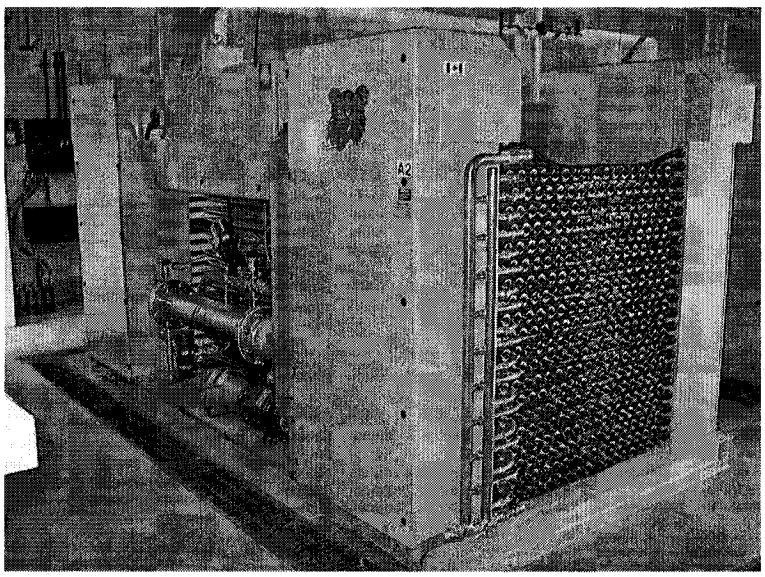

Figure 2.9: Purifics Photo-Cat® system [57]

2.4 Configurations Previously Studied

There have been numerous studies to overcome photocatalytic commercialization barriers by designing more efficient photoreactors. Table 2.1 shows a list of some photoreactor designs using titanium dioxide as a catalyst that have been presented in the literature and the important results found based on the configurations.

Table 2.1: Previously studied configurations

Configuration	Catalyst;Pollutant;Light	Important Results	Source
Annular	Membrane; formic acid & atrazine; Hg	Only small degradation rates achievable	[15]
Annular	Immobilized; phenanthrene & pyrene; UV	Reaction not mass transfer limited; rate independent of the feed concentration; low efficiency	[41]
Annular	Slurry; salicylic acid & phenol; blacklight & germicidal	265 nm radiation more effective than 350 nm; optimum rate with lower catalyst loading than required at 350 nm	[44]
Annular	Immobilized; 2-CP & 2-4-DCP; near-UV	Photo-CREC® reactor; catalyst decay and performance decay are main factors influencing conversion	[64]
Annular	Immobilized; *E. Coli* & formaldehyde; germicidal	Simultaneously perform photolytic sterilization and photocatalytic decomposition; low efficiency	[69]
Annular	Immobilized on silica beads; phenol; multiple UV	Best design is annular; performance limited by lamps; rate accelerated by H_2O_2	[77]
Beads	Immobilized on beads; *E. Coli*; UV	Muscovite beads better than glass beads, alginate beads, or quartz tube; air bubbling or H_2O_2 addition improves rate	[34]
Channel	Slurry; sodium formate; blacklight	Decomposition increased by 500 % with controlled periodic illumination	[61]

Continued on next page...

Table 2.1 – continued

Configuration	Catalyst;Pollutant;Light	Important Results	Source
Corrugated Fixed Plate	Immobilized; 4-CP & ammonia; UV	Faster and more energy efficient than flat plate; smaller angle more efficient; mass transfer higher than flat plate; potential to remove inhibitors from biological nitrification systems	[65, 85, 86, 87, 88]
Cylindrical	Slurry; phenol; solar	Concentrating radiation increased rate; photochemical phenol degradation rate higher than photocatalytic; presence of anions reduced degradation rate	[81]
Electrolytic	Immobilized and slurry; methylene blue & oxalic acid; high P Hg	Photoelectrocatalytic faster than photocatalytic or electrochemical oxidation; pseudo first-order kinetics	[5, 6, 7]
Electrolytic	Immobilized; 4-CP; Hg vapour	Photoelectrocatalysis improved efficiency over photocatalysis; reduced recombination reaction	[35]
Falling Film	Immobilized; microcystins; germicidal	Photocatalytic oxidation effective for destruction of microcystins; low pH improved rate; presence of radical scavengers detrimental	[67]
Falling Film	Immobilized; 2-CP, formetanate, pesticide mixture & dye mixture; solar	Multi-step reactor is as efficient as slurry; final filtration step eliminated	[73]

Continued on next page...

Table 2.1 – continued

Configuration	Catalyst;Pollutant;Light	Important Results	Source
Fixed Bed	Immobilized; phenol; UV	Packed bed has higher degradation than coated mesh; fixed bed is suitable for water decontamination	[23]
Fountain	Slurry; salicylic acid & indigo carmine dye; solar & UV	Large surface areas optimal; increasing feed and flow rate gives higher conversions	[55, 56]
Glass Fibres	Immobilized; 2-CP; high P Hg	Degradation 1.6 times higher than with slurry; TOC destruction 2.8 times faster	[30]
Glass Matrix	Immobilized; CP; 6 blacklights	Degradation follows first-order kinetics; modified L-H kinetics	[3]
Membrane	Immobilized on fibreglass cloth; 2-propanol; blacklight	Enhanced aeration provided by membrane separating gas and liquid increased photocatalytic activity without air bubbling	[78]
Multi-channel	Immobilized; dichlorobenzene & phentanthrene; Xe short arc lamp	More efficient than annular; higher catalyst surface area per volume; pseudo first-order kinetics	[41]
Multiple Tube	Immobilized; dye; low voltage halogen	Successful large scale reactor; efficient light distribution; high surface area to volume ratio	[58, 59]
Optical Fibre	Immobilized on optical fibre; tetrachloroethylene; UV LEDs	UV LED is a viable light source; very low light output to catalyst surface area necessary	[13]
Packed Bed	Immobilized; 1,2-dioxane; UV	Reaction is kinetics not mass transfer limited; UV light penetration substantial	[46]

Continued on next page...

Table 2.1 – continued

Configuration	Catalyst;Pollutant;Light	Important Results	Source
Rotating Disk	Immobilized; chlorinated VOC & 3,4-dichlorbut-1-ene; UV	Rate increases as rotational speed increases; minimal effect of oxygen partial P; rate increases with light intensity; rate increases at low pH	[27]
Rotating Disk	Immobilized; phenol, chlorinated phenols, 4-chlorobenzoic acid & lindane; near-UV	Rotating disk attractive option; similar degradation rates at different angular velocities; no significant mass transfer resistance; degradation rate increases with concentration; linear dependence on light intensity; L-H kinetics	[17, 18, 19]
Rotating Drum	Pt-loaded immobilized; phenol; solar & Hg	L-H kinetics; high photoefficiency; Pt improves efficiency; aeration did not improve rate; critical rotational speed 25 rpm; degradation rate high with solar light, but higher with mercury lamp	[83]
Spinning Disc	Immobilized; 4-CP & salicylic acid; UV	Lamps with shorter wavelength more efficient; coating technique unsuitable	[80]
Taylor Vortex	Immobilized and slurry; dyes (Orange II, Eosin B, SSB), benzoic acid & phenol; UV	Promising for water purification; no significant rate difference for immobilized and slurry; more efficient than multiple tube	[21, 63]
Tubular	Immobilized; Special Brilliant Blue; U-shaped UV	All advantages of multiple tube reactor; easily scalable; catalyst activated at highest level	[58]

Continued on next page...

Table 2.1 – continued

Configuration	Catalyst;Pollutant;Light	Important Results	Source
Tubular	Immobilized; phenol & methylene blue dye; UV	Immobilized catalyst has less activity than powder; H_2O_2 addition enhanced activity; higher light intensity results in higher rate; adsorption favoured at higher pH; no effect of temperature	[42]
Tubular	Immobilized Pt-loaded; phenol, tetrachloroethylene & bisphenol A; UV	High efficiency; simple design; aeration is necessary for continuous; L-H kinetics; rate faster as flow increases	[84]

Three of the successful reactor configurations presented in the previous table are considered in further detail as they were used as a basis for the proposed reactor design.

2.4.1 Corrugated plate

Studies by Zhang et al. [85, 87, 88] and Shang et al. [65] consider a titanium dioxide coated corrugated plate reactor for the degradation of 4-chlorophenol and ammonia under ultra-violet lamps and found very promising results in enhancing the energy efficiency of photoreactors. This reactor configuration is shown in Figure 2.10.

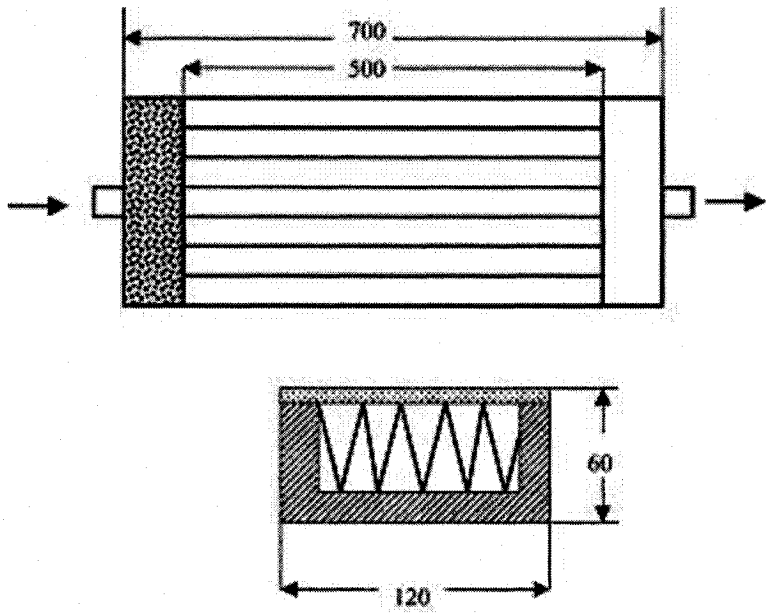

Figure 2.10: Corrugated plate reactor [88] — top view and cross-section

Experimental analysis of a continuous corrugated plate reactor system with 30 mg/L of 4-chlorophenol [88] showed that corrugated plate reactors were up to 150 % faster than flat plate reactors given similar dimensions and had degradation rates comparable to a 1 g/L slurry reactor, the electrical energy was estimated to be near that of a slurry system and the mass transfer rates were found to be 400 % to 600 % higher than flat plate reactors [88]. In addition, significant analysis of the corrugation angle indicated

that decreasing the angle, and thereby increasing the surface area and the number of corrugations, enhanced the rate of degradation for the range of angles studied (7°, 10°, 14°, 20° and 40°). These benefits are due to the enhanced surface area and ability to deliver photons and reactants to the reactor surface. In addition, Langmuir-Hinshelwood kinetics was found to be applicable for such a reactor system.

Extensive modelling and experimental validation of a corrugated plate reactor configuration using a local-area-specific rate of energy absorption (LASREA) distribution indicates that a smaller corrugation angle is more efficient because it recaptures reflected light photons, but it does not have a uniform adsorption rate across the plate [65, 85, 87].

Finally, analysis was completed of the corrugated plate reactor system for the pre-treatment of groundwater contaminated with ammonia and other compounds as an alternative to carbon adsorption [86]. Although further analysis is necessary, the corrugated photoreactor showed promising results for this pre-treatment — up to 60 % of the ammonia nitrogen was nitrified.

2.4.2 Rotating Disks

Hamill et al. [27] studied a rotating disk photocatalytic reactor comprised of four glass rotating disks immobilized with titanium dioxide and ultra-violet lamps mounted between the discs (see Figure 2.11). This reactor design showed degradation rates approaching that of a slurry reactor (0.0242 min^{-1} for the rotating disc reactor and 0.0330 min^{-1} for the slurry reactor). A step-wise increase in degradation rate was found for rotational speeds from 0 rpm to 136 rpm due to changing mass transfer properties of the system with changing rotational speeds. Little effect of oxygen concentration was found except at very low concentrations, therefore the dissolved oxygen in the system is not limiting for the conditions studied. The effect of light intensity at two rotational speeds (20 rpm

and 136 rpm) was studied — at 20 rpm there was an increasing degradation rate with increasing intensity up to 2 mW/cm^2 and no further increase was observed; however, at 136 rpm the degradation rate continued to increase with increasing intensity within the entire range of intensities studied (0 mW/cm^2 to 6 mW/cm^2). Finally, the effect of pH was studied indicating that a 23 % increase in degradation rate constant was found by lowering the pH of the system from 4.6 to 2.

A similar reactor configuration studied by Dionysious et al. [18] with one titanium dioxide coated rotating stainless steel disk (Figure 2.12) and a continuous experimental set-up with phenol, chlorinated phenols and lindane as the model pollutants. No changing degradation rates with rotational speeds of 12 rpm to 25 rpm were observed due to a lack of mass transfer limitation in the system. In addition, an increasing degradation rate following Langmuir-Hinshelwood kinetics was observed for 2,4,6-trichlorophenol concentrations from 25 ppm to 206 ppm. However, this increase was accompanied by a decrease in the pollutant removal efficiency.

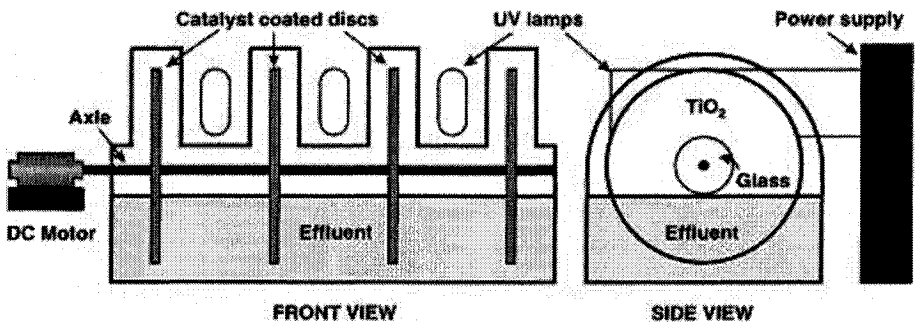

Figure 2.11: Four rotating disks reactor [27]

2.4.3 Rotating Drum

A study by Zhang et al. [83] considers a photocatalytic reactor with a platinum-loaded titanium dioxide coated rotating glass drum (see Figure 2.13) for the degradation of

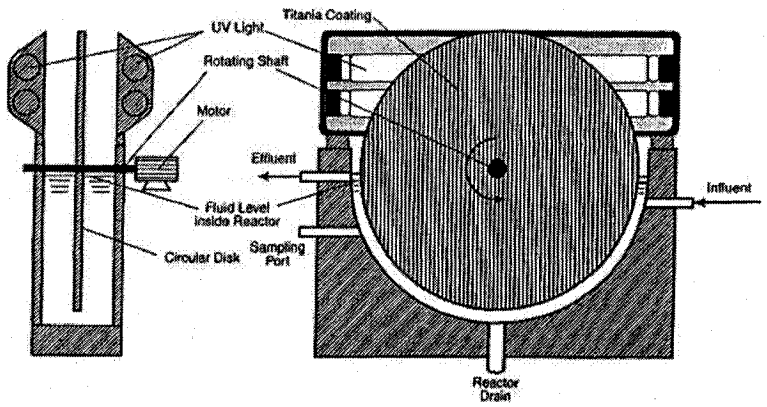

Figure 2.12: Single rotating disk reactor [18]

22 ppm of phenol. Using this reactor design for 25 mL of contaminated medium and 25 rpm, the phenol was degraded to undetectable concentrations within one hour under solar light. This degradation is much slower than that when two 6 W mercury lamps are used (1.635 mg/m^2 for solar light and 4.88 mg/m^2 for mercury lamps). Loading the titanium dioxide catalyst with platinum was found to increase the degradation rate by about 75 %. Finally, considering rotational rates of 5 rpm, 25 rpm and 55 rpm, there was an increase in degradation rate between the 5 rpm and 25 rpm runs, but not between the 25 rpm and 55 rpm runs.

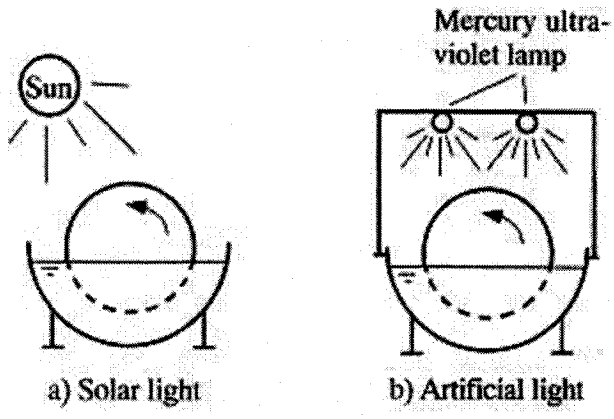

Figure 2.13: Rotating drum reactor under solar and mercury light [83]

Chapter 3

Proposed Photoreactor Configuration

In this work, a novel photocatalytic reactor is proposed. The reactor system is comprised of a titanium dioxide coated rotating drum with a corrugated surface that is partially immersed in a phenol and distilled deionized water solution with an ultra-violet light source to illuminate the drum from above.

A corrugated surface was chosen for the reactor drum to increase the available surface area for catalyst immobilization, to exploit the potential to recapture reflected light and to improve the mass transfer of polluted water to the reaction sites. The main benefit of adding rotation to the drum is to continuously transfer reactants to the catalyst surface and products to the reaction medium. In addition, the rotation also takes advantage of periodic illumination effects which have been shown to decrease amounts of reaction intermediates in the system and promote organic compound oxidation. The combination of the rotation and the corrugated surface also enhances the agitation in the system which is beneficial in maintaining a completely mixed reactor system and adding dissolved oxygen to the reaction medium.

Several drums of different corrugation configurations were studied primarily to determine the effects of the additional surface area and the configuration design. Three of the drum configurations have angled corrugations with different angles that are used to compare the effect of corrugation angle and surface area. Three other drums have a finned configuration instead of angled with different numbers of fins equi-spaced around the reactor drum. These drum configurations were compared to each other and to the base-case of a non-corrugated rotating drum reactor.

In addition to the effects of surface area and drum configuration, the effects of rotational speed, initial pollutant concentration and illumination intensity were considered. Finally, the reaction kinetics and the reproducibility of the reactor system were studied. This study is intended to facilitate the design of reactor systems by providing a unique drum configuration with higher organic pollutant degradation rates than those of typical photocatalytic reactors.

Chapter 4

Materials and Methods

The following sections reveal the materials used for these experiments including the chemicals and reactor equipment, and discuss the methods used including the catalyst immobilization, system start-up, experimental procedure and analysis techniques.

4.1 Chemicals

The catalyst for these experiments is Aeroxide® P25 titanium dioxide from Degussa Corporation (New Jersey, United States) which has an average particle size of 30 nm. To immobilize the catalyst on the reactor drums, a standard slurry of 180 g/L TiO_2 was prepared by dispersing the TiO_2 powder in an aqueous solution of 25 % methanol by volume (Optima® 99.9 %, Fisher Chemicals, Ontario, Canada) in distilled deionized water.

The model pollutant used for the experimental runs was 99.9 % phenol from Sigma-Aldrich Inc. (Missouri, United States). For the experimental runs, an approximately 20 mg/L (5 mg/L or 40 mg/L for initial concentration experiments) solution of phenol in distilled and deionized water was used.

Finally, for the HPLC analysis, HPLC grade acetonitrile and phosphoric acid from Fisher Chemicals (Ontario, Canada) were used as the mobile phase. The mobile phase was 49.575 % acetonitrile, 50 % distilled deionized water and a buffer of 0.425 % phosphoric acid (by volume).

4.2 Reactor Equipment

The experimental apparatus (not including the illumination source) used is depicted in Figure 4.1. The 2.09 L (21.59 cm x 15.24 cm x 6.35 cm) reactor tank and drums were constructed in-house from stainless steel. The tank is a double-walled container that allows cooling water to flow between the walls without contaminating the reaction medium, while maintaining the temperature of the reaction medium at approximately 10 °C.

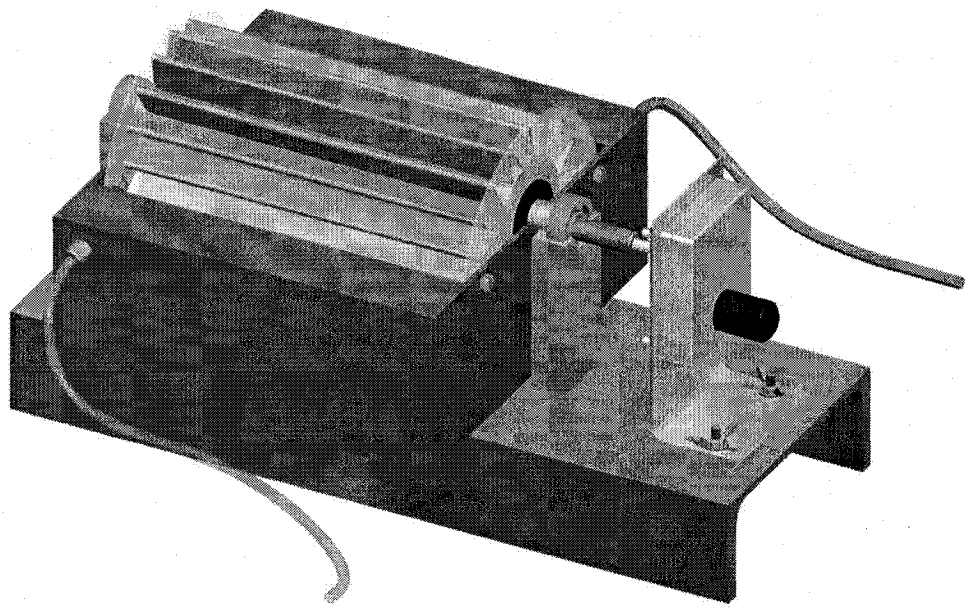

Figure 4.1: Experimental apparatus for photocatalytic contaminant degradation

The reactor tank holds a drum partially immersed in the reaction medium for the

Table 4.1: Available catalyst immobilization surface area

Drum Configuration	**Surface Area** (cm^2)
No Corrugations	405
16 Fins	1704
28 Fins	2679
40 Fins	3653
30° Angle	1164
20° Angle	1402
10° Angle	2411

experiment. The drums were made from 6.35 cm diameter and 20.32 cm long stainless steel cylinders, and the corrugations on the drums were made from 0.08 cm thick stainless steel and are 2 cm high. As shown in Figure 4.2, the seven drum configurations used are (a) no corrugations, (b) sixteen fins, (c) twenty-eight fins, (d) forty fins, (e) thirty degree angle, (f) twenty degree angle and (g) ten degree angle. The surface area available for catalyst immobilization for each of the drums is shown in Table 4.1. In addition to affecting the number of available reaction sites, the surface area also affects the total amount of contaminant that is on the drum surface during the rotational cycle and the ability of the drum to recapture reflected light.

The illumination source used to activate the catalyst consists of three Philips Actintic mercury 40 W reflector blacklights (TLK 40W/10R UV-A) from Microlites Scientific (Ontario, Canada) with an average wavelength of 353 nm. Each of the light tubes was 58.42 cm long and 3.81 cm in diameter, and they were positioned 3.18 cm from the edge of the drum corrugations with the middle tube centered on the drum and the other tubes spaced 1.91 cm on either side of the center tube. The position of the lights in relation to the reactor drum is shown in Figure 4.3. The support for the lights and the reactor cover were also made in-house of stainless steel.

The drums were rotated with a Dayton parallel shaft 12 V DC gear-motor with a nameplate speed of 50 rpm from Acklands-Grainger (Ontario, Canada) and the rotational

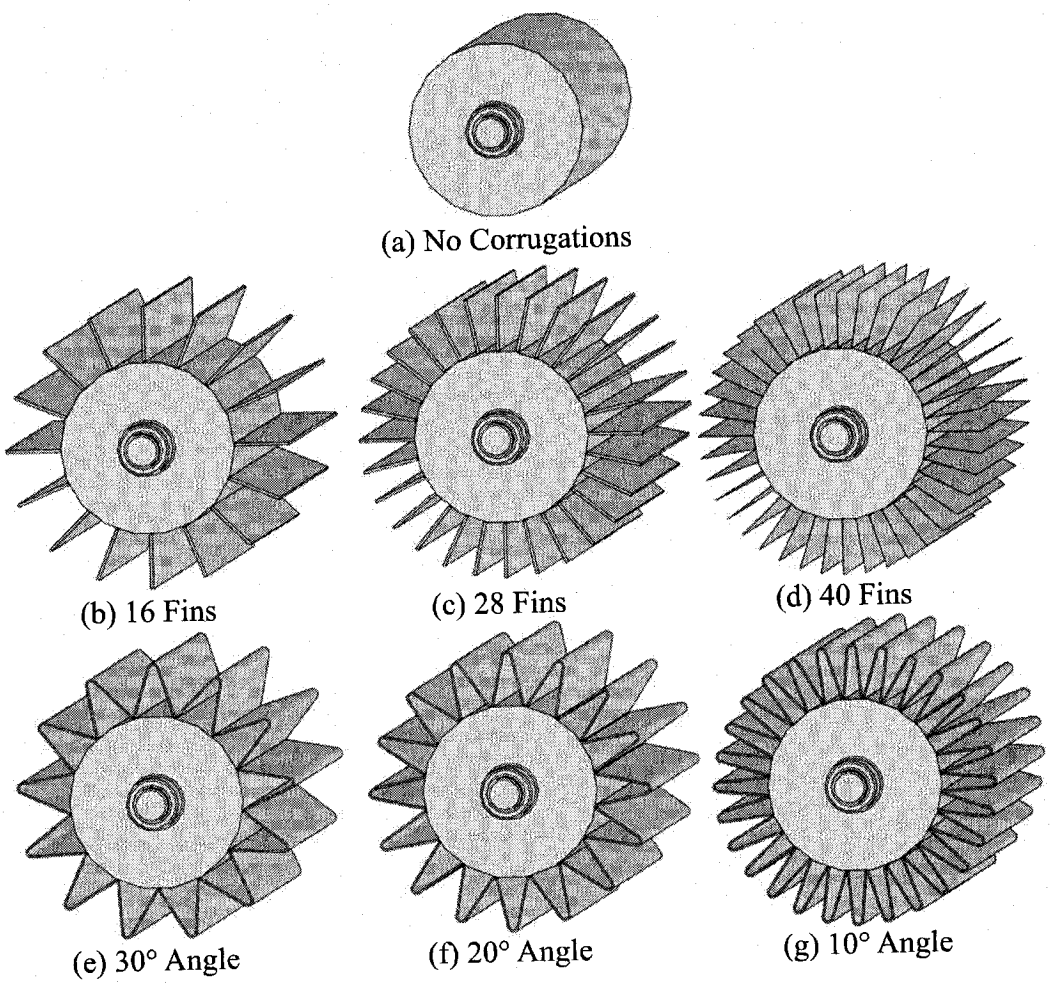

Figure 4.2: Reactor drum configurations for photocatalysis experiments

speed was controlled with a variable DC power supply from EPSCO Inc. (Illinois, United States).

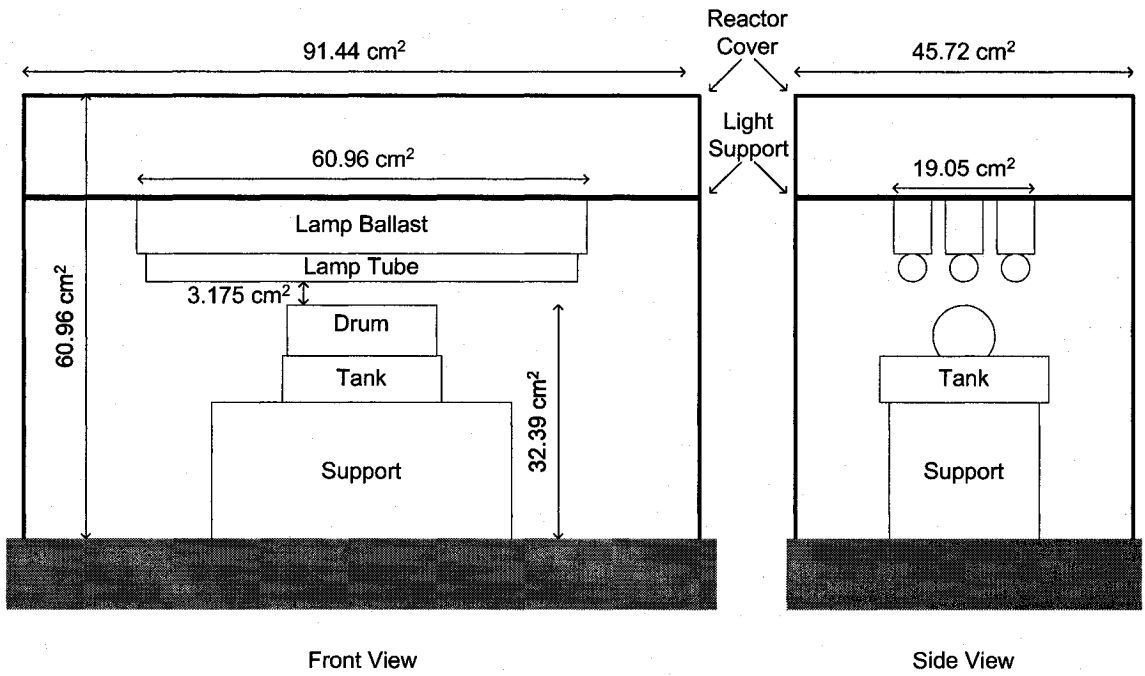

Figure 4.3: Schematic representation of experimental apparatus

4.3 Catalyst Immobilization

In preparation for catalyst immobilization, each of the drums was cleaned with liquid detergent (Liqui-Nox, Alconox, New York, United States) and rinsed with distilled water. They were then heated to 200 °C for two hours. Upon cooling at room temperature, a thin coat of the TiO_2 slurry was applied evenly to the drums and they were dried at 275 °C for five hours to immobilize the titanium dioxide. After cooling again at room

temperature, the drums were then rinsed with distilled water to remove any detached TiO_2 before commencing the experimental runs.

4.4 System Start-Up

Before each experimental run, the reactor tank and drum were rinsed with distilled water to remove any detached TiO_2 and residual reactants, intermediates and products. The flow of cooling water was turned on, the drum was installed in the reactor tank and the drum rotation was initiated. When the water temperature and the rotational speed stabilized (approximately ten minutes), 1.25 L of reaction medium (solution of phenol and distilled deionized water) was added to the reactor tank. Finally, the illumination source was turned on and, thus, the reaction was initiated.

4.5 Experimental Procedure

After completion of the system start-up procedure, the reaction continued until there was less than a 3 % change in pollutant concentration over a sixty minute period. During this time (approximately six hours), samples were taken every thirty minutes and analysed for pollutant concentration with the spectrophotometer. Where necessary, the samples were kept for subsequent HPLC analysis. The rotational speed and the reaction medium temperature were also monitored regularly throughout the experimental run to ensure that there was no substantial change in either parameter during that run.

4.6 Analysis Methods

The samples taken during the photoreactor experimental runs were analyzed for absorbance with a GENYSYS 10-UV Spectrophotometer from Geneq Inc. (Quebec, Canada). Prior to starting the experimental runs, the scanning function on the spectrophotometer was used with a standard solution of 20 mg/L phenol and distilled deionized water to determine that the highest absorbance peak for phenol occurred at a wavelength of 209 nm. Subsequently, a calibration curve for the range of concentrations used in the experiments was developed (Figure A.1). Each of the samples was analyzed using the 209 nm wavelength and the calibration curve. The spectrophotometer was recalibrated monthly to ensure that there was no substantial drift in the measurements.

Some of the experimental runs were analyzed with the HPLC in addition to the spectrophotometer to determine the effect of UV-absorbing reaction intermediates. The samples and a set of standards were tested starting from low concentrations to high concentrations with double injections of 5 μL each to ensure that the most accurate results achievable were obtained from the HPLC. The HPLC unit consists of a Waters 486 Tunable Absorbance Detector, 600E System Controller and 717 Autosampler. The mobile phase used was 49.575 % acetonitrile and 50 % distilled and deionized water with a 0.425 % phosphoric acid buffer (by volume). All samples were analyzed at a wavelength of 210 nm because this is the literature wavelength of maximum absorption for phenol. As with the spectrophotometer, a calibration curve for the HPLC was also developed (Figure B.1).

Chapter 5

Results and Discussion

Experimental runs were completed to assess the effects of various reactor parameters on the photodegradation rate. Before beginning the actual experimental runs, control runs were completed to ensure that there was no pollutant degradation without the catalyst, lights and rotation all present. The first set of experimental runs was completed to determine the reproducibility, and thus the reliability, of the experimental data. Next, various runs were completed to determine the effects of drum configuration, rotational speed, illumination profile and initial pollutant concentration. HPLC analysis was completed to analyze the presence of reaction intermediates. Finally, the applicability of Langmuir-Hinshelwood kinetics for this photoreactor system was considered.

Each experimental run had a pollutant degradation trend similar to that shown in Figure 5.1 for the 16 fin drum at 15 rpm and an initial phenol concentration of 20 ppm. As shown, the initial degradation rate is equal to the slope of the trend-line for the zero order (linear) portion of the data.

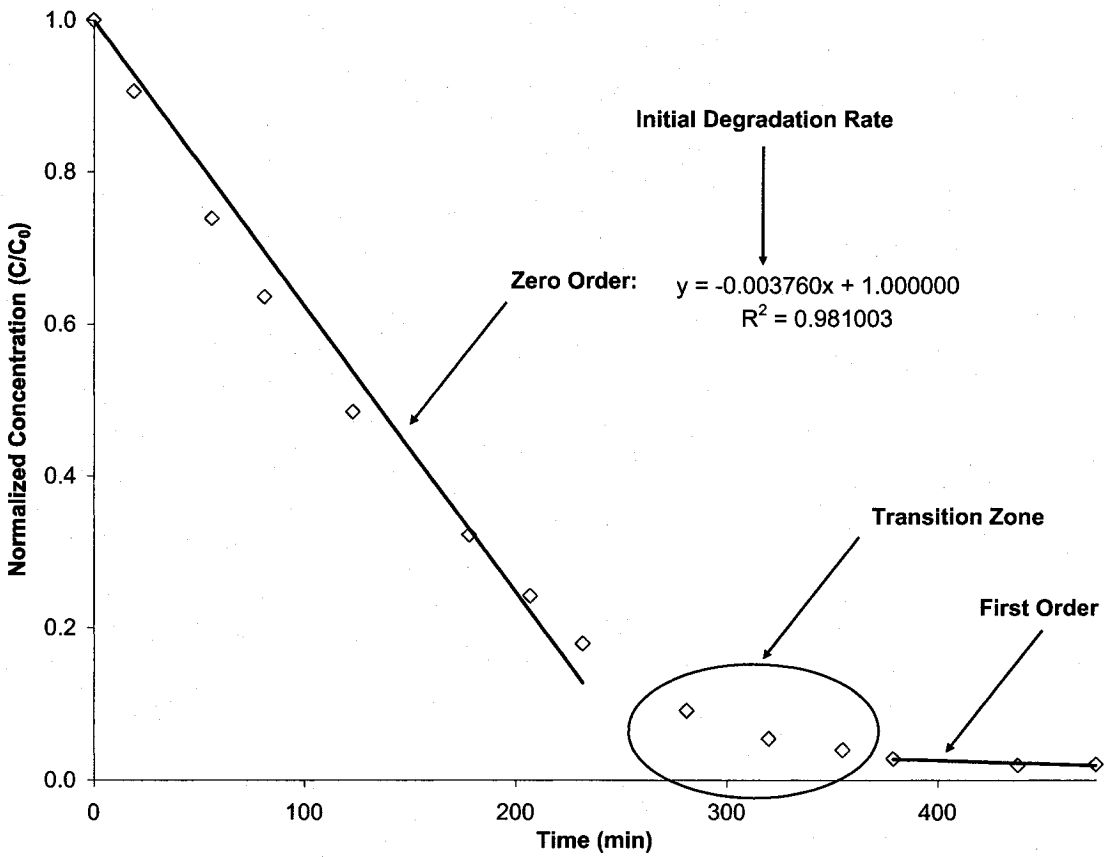

Figure 5.1: Example pollutant degradation trend for photocatalysis run

5.1 Control Runs

Five control runs were completed using the 28 fin drum configuration, to determine whether phenol degradation occurs under other conditions than photocatalytic. As indicated in the Table 5.1, the only phenol degradation occurs with all factors present — the catalyst, illumination and rotation. Therefore, this system operates purely under photocatalytic degradation.

Table 5.1: Control run experimental results

Run	Catalyst	Lights	Rotation	Phenol Concentration		Time
				Initial (ppm)	Final (ppm)	
1	none	off	on	24.71	24.90	332 min
2	none	on	on	24.07	24.59	323 min
3	present	off	on	25.76	24.86	341 min
4	present	on	off	21.42	21.76	330 min
5	present	on	on	23.56	3.29	325 min

5.2 Reproducibility

A series of tests were completed to determine the reproducibility of the degradation rates obtained from the experimental runs. Figure 5.2 shows degradation rates from the experimental runs for the 20° angle drum and the 28 fin drum with the same operating conditions (20 ppm initial concentration, 15 rpm rotational speed and all three lights on). A slight decrease in the degradation rate as the runs progress due to catalyst detachment during the experiments is expected. As shown in Figure 5.2, the first run has a very high degradation rate (20° drum) and the sixteenth run has a very low degradation rate (28 fin drum). The decrease after the first run was also observed with the other drums as there is substantial catalyst detached during the first run, but minimal detachment during the additional runs.

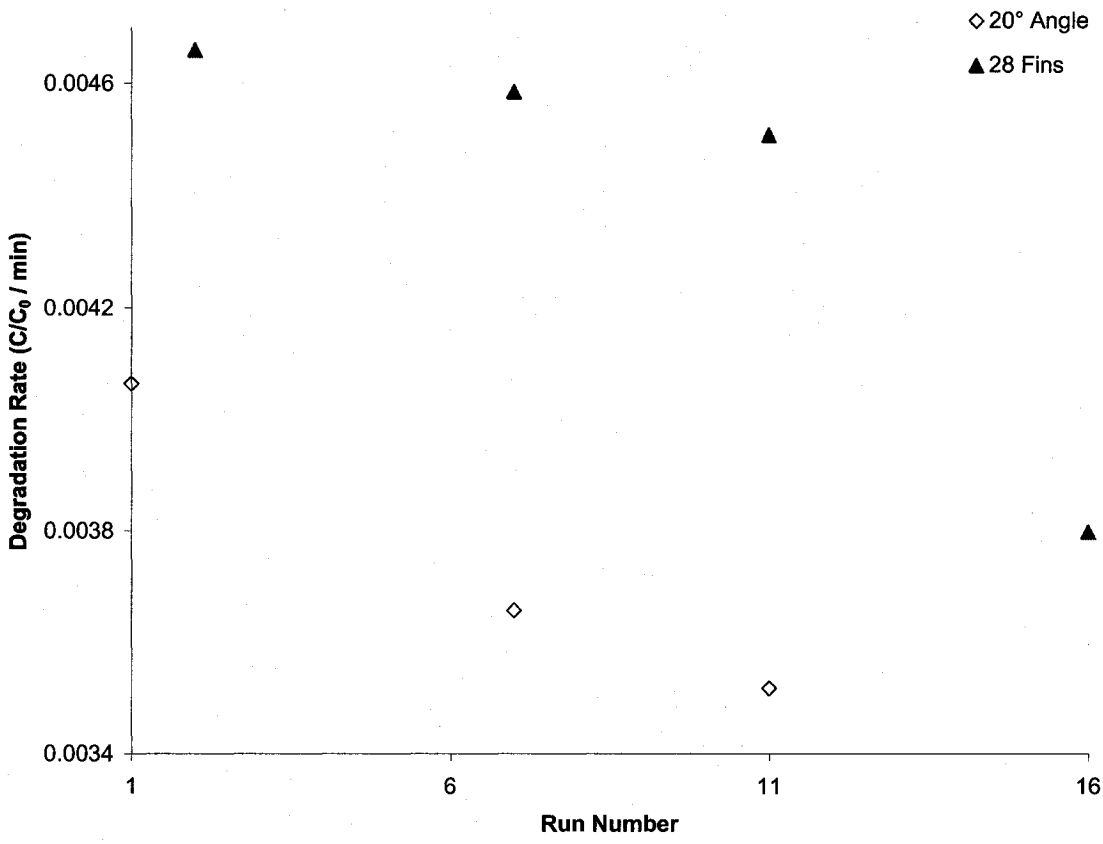

Figure 5.2: Reproducibility of degradation rates at 15 rpm and 20 ppm

Table 5.2: Sample mean and standard deviation for reproducibility tests

Drum	Data	Sample Mean	Standard Deviation
20° Angle	1 - 11	0.00375	0.00028
20° Angle	2 - 11	0.00359	0.00010
28 Fins	2 - 16	0.00439	0.00040
28 Fins	2 - 11	0.00458	0.00008

Table 5.2 shows the sample means and standard deviations for the data in Figure 5.2 including all runs and just including the second to eleventh runs, i.e. omitting the first run for the 20° drum and the sixteenth run for the 28 fin drum. The magnitude of the variances shows that the data are much more reproducible without including the first run or the sixteenth run. Therefore, to maintain consistency in the experimental data, results were only compared between the second and eleventh experimental runs (inclusively) as this range shows the best data reproducibility. The standard deviation for the initial degradation rate used to calculate the standard error in the following graphs is taken as 0.0001 min^{-1}.

5.3 Drum Configuration

An extensive study of the effect of drum configuration on the phenol initial degradation rate was completed. Although there is significant scatter in the data, Figure 5.3 shows an increasing trend of initial degradation rate (C/C_0/min) with increasing surface area. There is approximately a 200 % increase from the degradation rate of the lowest surface area drum (no corrugations) to that of the highest surface area drum (40 fins). Because the configurations with higher surface areas have an increased amount of catalyst and, therefore, more reaction sites, the degradation rate tends to increase with increasing surface area. This trend is consistent with that found in experimental studies using corrugated plate reactors [85].

The graph in Figure 5.4 shows that there is generally a decreasing trend of degradation rate with increasing surface area on a unit surface area basis (65 % decrease from the non-corrugated drum to the 40 fin drum). This indicates that the drum configurations with high surface areas do not make efficient use of that surface area. This phenomenon is expected because with a higher surface area the illumination intensity per unit surface

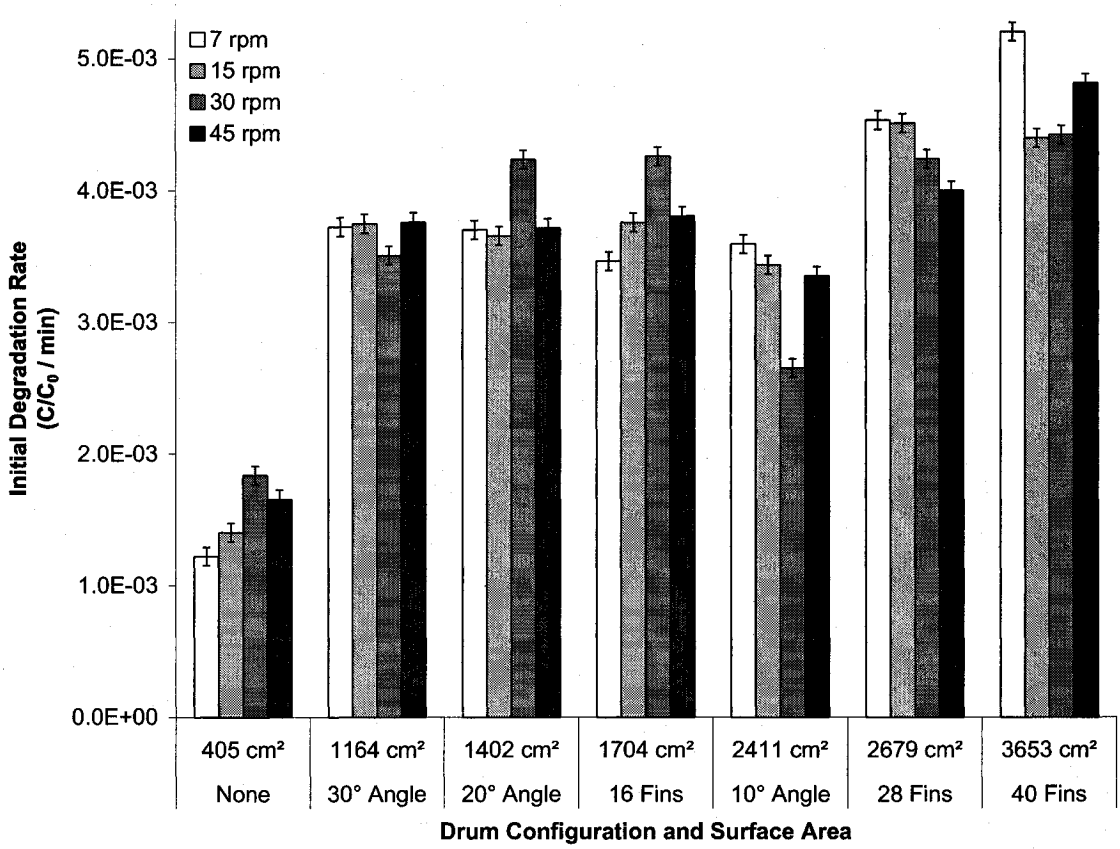

Figure 5.3: Effect of drum configuration and its surface area on degradation rate

area decreases. Thus, the surface area unit intensity of the illumination decreases when additional surface area is added to the drum configuration. As previously reported, the degradation rate is expected to decrease with decreasing light intensity which supports the observed results.

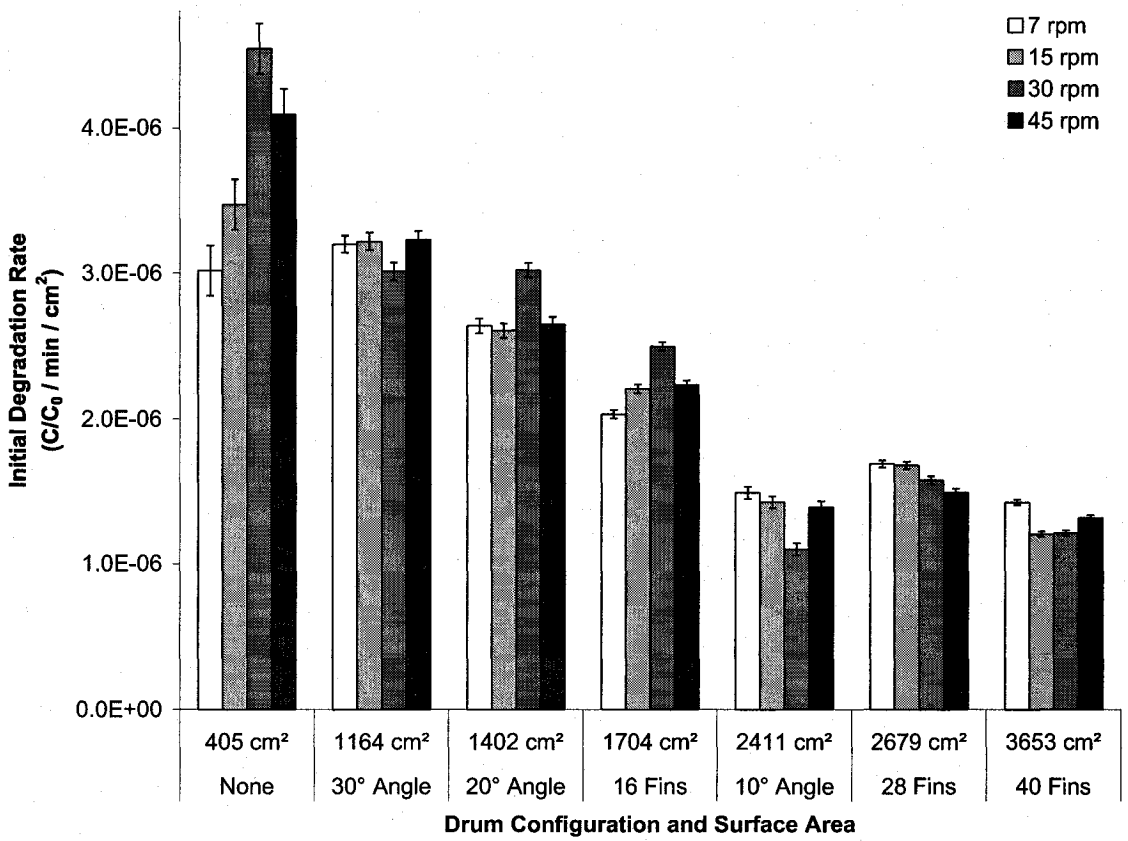

Figure 5.4: Effect of drum configuration on unit surface area degradation

5.4 Rotational Speed

Figures 5.5 and 5.6 show the effect of rotational speed on the phenol initial degradation rate for the drums with angled corrugations and finned corrugations respectively. There is no distinguishable trend of the effect of rotational speed on the degradation rate

when considering a range of rotational speeds from 0 rpm and 45 rpm. Therefore, these results are not consistent with the previously reported results that demonstrate a critical rotational speed of 25 rpm for a rotating drum photoreactor to degrade 25 mL of a 22 ppm phenol solution [83]. However, they are consistent with the results observed by Hamill et al. [27] that indicate step-wise increases in degradation rates with increasing rotational speeds.

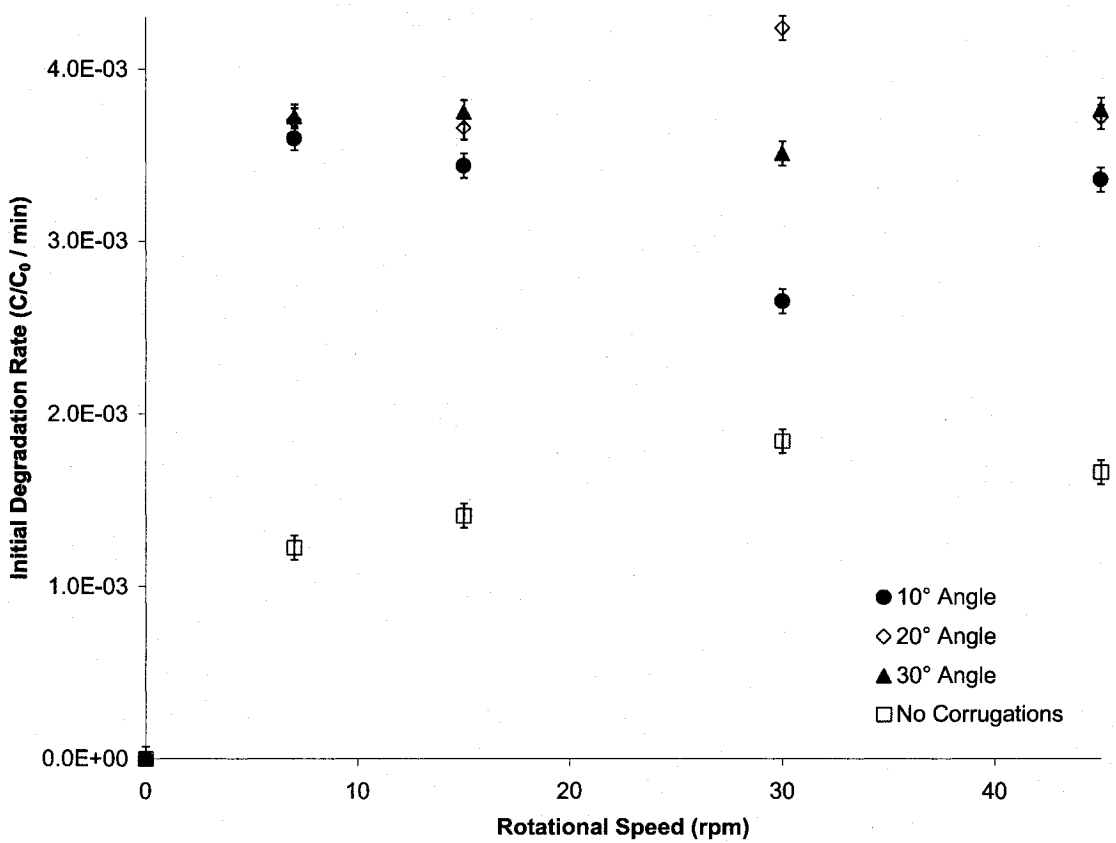

Figure 5.5: Effect of rotational speed on degradation for angled drums at 20 ppm

Since higher rotational speeds have improved transfer of reactants to the catalyst surface, the lack of distinct correlation between the rotational speed and the degradation rate indicates that the reaction is not limited by mass transfer at 20 ppm. However, no conclusion as to the exact effect of rotational speed on the degradation rate can be made

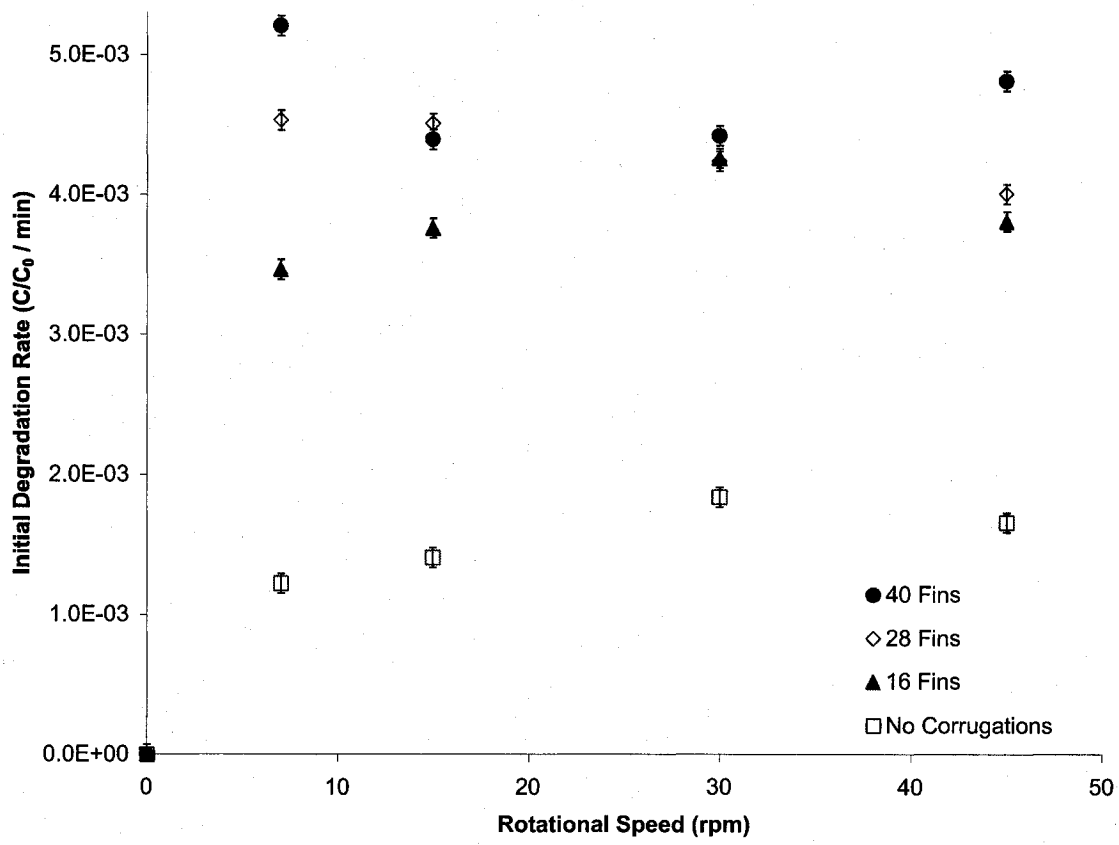

Figure 5.6: Effect of rotational speed on degradation for finned drums at 20 ppm

from these experimental data.

5.5 Initial Pollutant Concentration

A study of the effect of initial phenol concentration at different rotational speeds using the 28 fin drum was conducted. For this comparison, the initial degradation rate was not normalized to the initial concentration so that a comparison of the actual degradation rates at the different initial concentrations could be made. As shown in 5.7, the results are consistent with the reported literature [45, 44] and Langmuir-Hinshelwood kinetics — at low concentrations (5 ppm to 20 ppm) there is an increase in degradation rate with increasing initial concentration, but high concentrations (20 ppm to 40 ppm) no further improvement in degradation rate is observed.

In addition, at 5 ppm there is a dependence of reaction rate on rotational speed — the degradation rates at 30 rpm and 45 rpm are 76 % higher than those at 7 rpm and 15 rpm. The dependence of degradation rate on rotational speed at 5 ppm and the increase in degradation rate between the 5 ppm and 20 ppm experiments indicate that at such a low concentration (5 ppm) the reaction is limited by the ability to transfer reactants to the catalyst surface. Conversely, at 20 ppm and 40 ppm the lack of significant increase of degradation rate with increasing rotational speed or initial concentration indicates that the reaction is limited by the reaction kinetics at these conditions.

5.6 Illumination Profile

A brief study of the effects of illumination profile on the degradation rate of phenol in the photoreactor was completed. The lights used for each experiment are positioned differently (see Figure 5.8) — for the run with three lights the lights were centered on

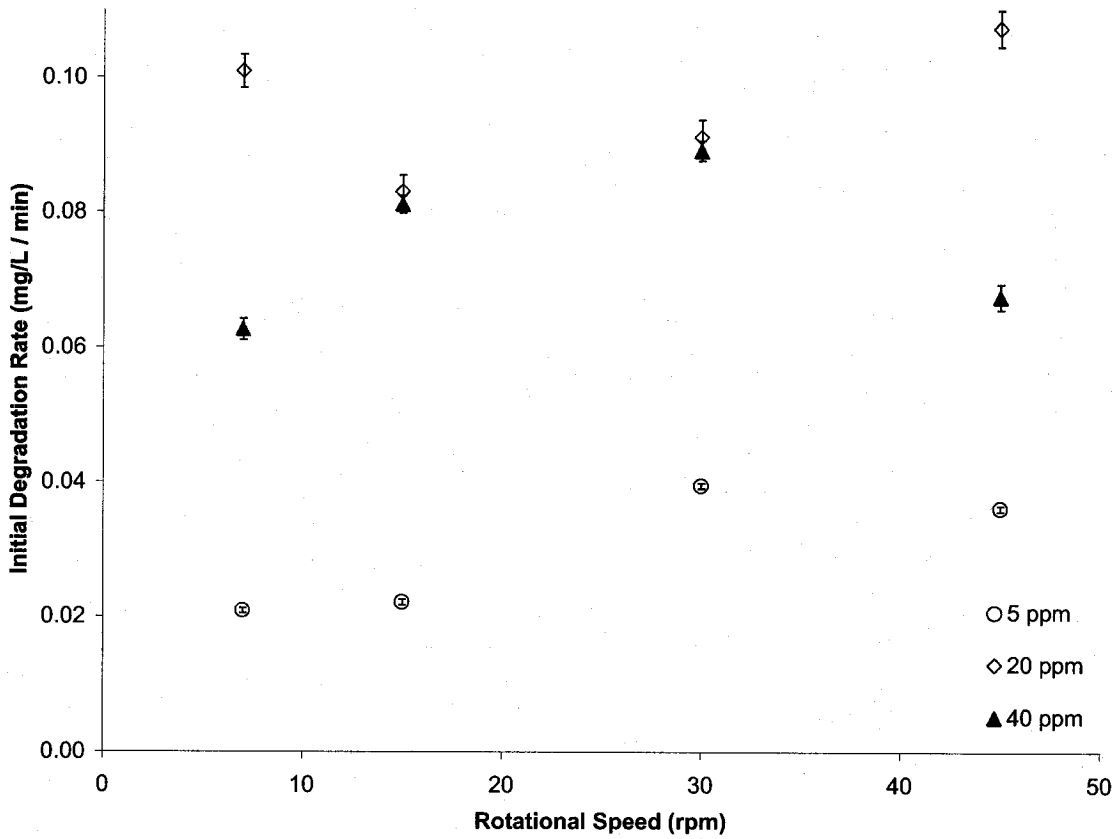

Figure 5.7: Effect of initial concentration on the degradation rate for 28 fin drum

the drum, for the run with two lights just the two outside lights were used and for the run with one light just the middle light was used.

As shown in Figure 5.9 the degradation rate using two ultra-violet lamps is 19 % higher than the run using a single lamp, while the degradation rate using all three lamps is 73 % higher than that using one lamp. The large difference between the degradation rate with two lights and that with three lights is expected because of the position of the lights. In the run with all three lights, the middle light was added which is closer to the drum and thus provides light with a stronger intensity giving an increase in degradation rate of 45 % over the two light configuration. From Figure 5.9 it is evident that, as indicated in the literature [51], the degradation rate does increase with increasing light intensity for this reactor configuration. However, because this experimental design couples the effects of light intensity and radiation pattern, it is not conclusive as to the exact effect of either parameter independently.

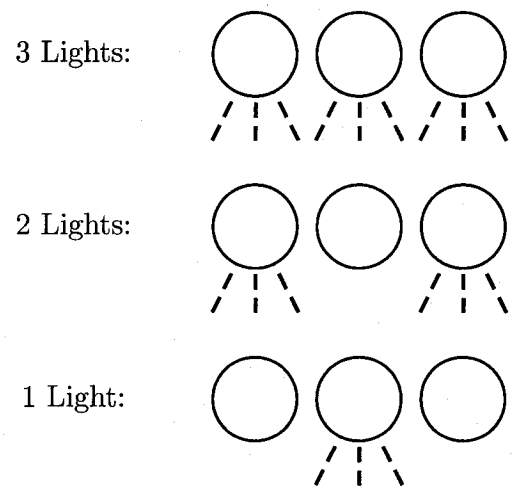

Figure 5.8: Configuration of lights for illumination profile runs

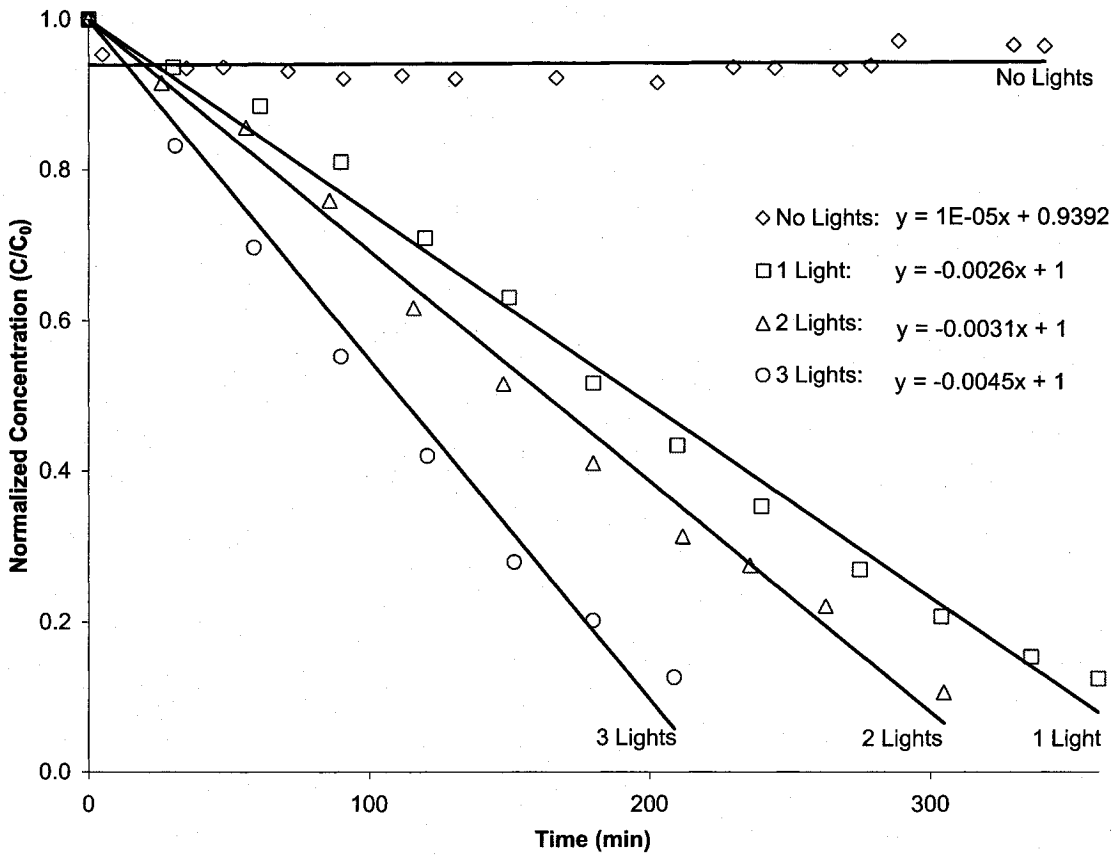

Figure 5.9: Effect of light intensity on the phenol degradation rate

5.7 Reaction Intermediates

For several experimental runs, the samples taken were analyzed with the HPLC as well as the spectrophotometer. Figure 5.10 shows a comparison of the HPLC concentrations and the spectrophotometer concentrations for a run with the twenty-eight fin drum at a rotational speed of 15 rpm and all three lights on. As shown in this graph, the HPLC concentrations are lower than the spectrophotometer concentrations which indicates the presence of reaction intermediates in the system. Since the same trend exists in both curves, the ultra-violet light absorbing reaction intermediates have minimal interference with the experimental data.

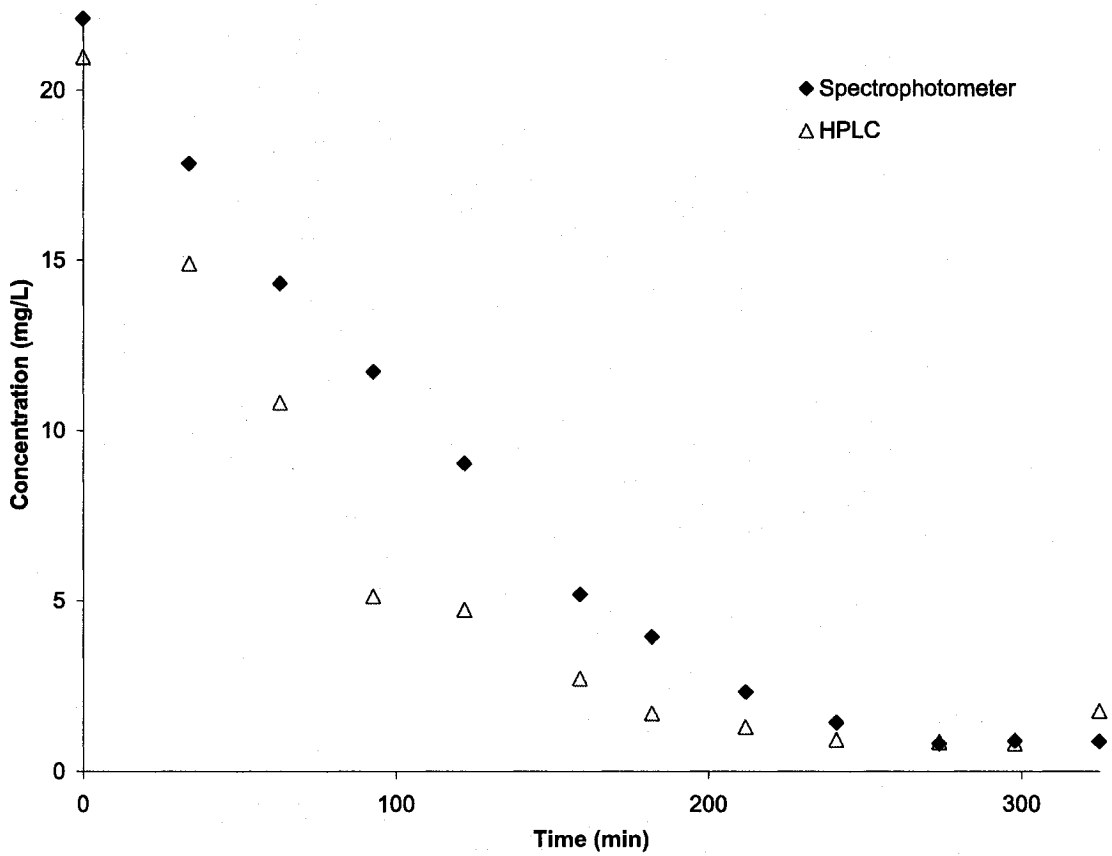

Figure 5.10: Comparison of HPLC and spectrophotometer concentrations

Figure 5.11 follows the absorbance of unknown compounds in the system as indicated by the HPLC chromatograms. Three main reaction intermediates were evident from the chromatograms; their retention times are 2.98 minutes, 3.20 minutes and 3.98 minutes and phenol has a retention time of 6.04 minutes. As shown in the previous graph, the interference of the reaction intermediates is minimal. However, there is an increased reaction intermediate presence at the end of the experiment that is not evident from the previous graph.

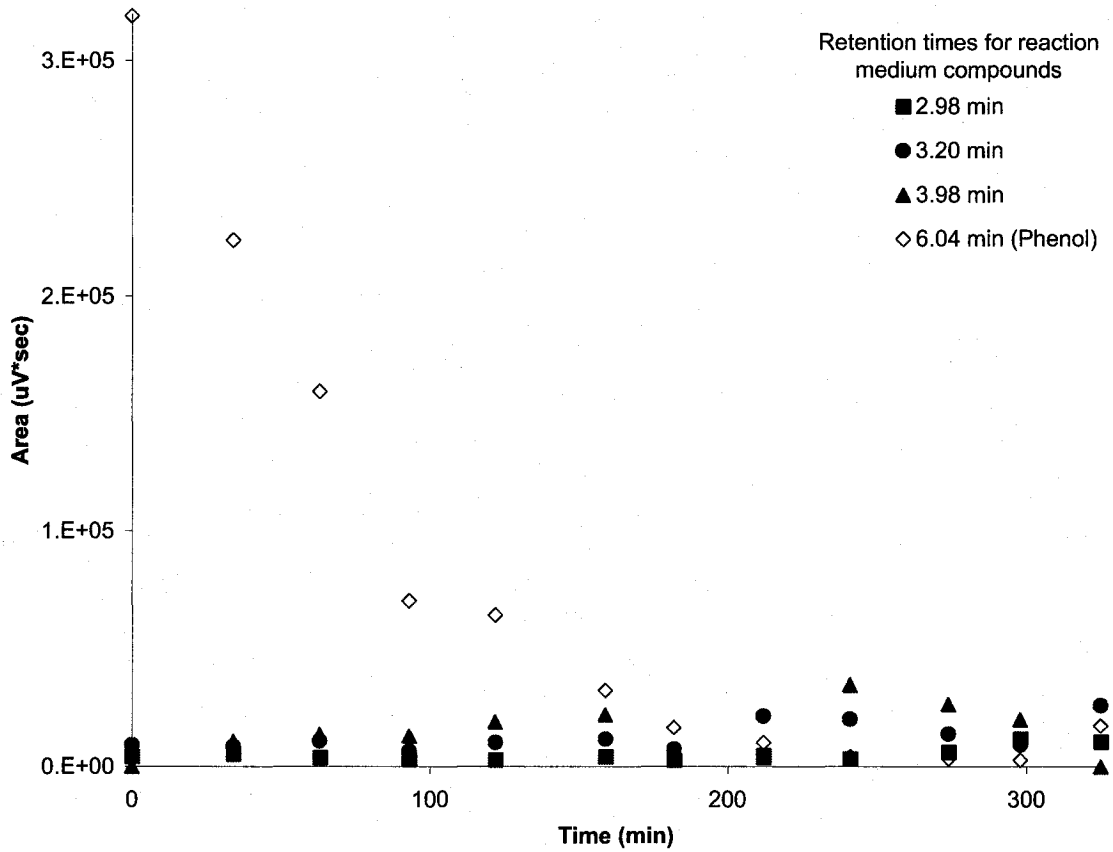

Figure 5.11: Reaction intermediates from HPLC analysis

5.8 Reaction Kinetics

Using the Langmuir-Hinshelwood (L-H) kinetics equation presented in Section 2.1.2 and shown below, the kinetics of the photocatalytic reactions were examined for each of the drum configurations at 15 rpm.

$$\frac{-dC}{dt} = \frac{k_r K C}{1 + KC}$$

The first step of this study was to find an appropriate average adsorption coefficient for phenol. This was achieved by minimizing the difference between the experimental $-dC/dt$ and that found using the kinetics relationship presented in Equation (2.3) by changing the values of the kinetic constants. The average adsorption coefficient of phenol found was $K = 0.120$ L/mg. Next, using the same methodology, but only changing the value of the overall reaction rate constant (k_r), the optimal value for k_r was determined for each drum configuration. Two graphs showing the applicability of Langmuir-Hinshelwood kinetics for the experimental data are shown below (Figures 5.12 and 5.13), while the remaining graphs are in Appendix C (symbols represent experimental data and lines represent kinetics data).

In addition, the values for k_r were compared to the surface area for catalyst immobilization for the drums to determine if there is any correlation between the surface area and the overall reaction rate constant. As shown in Figure 5.14, there is an increasing trend of overall reaction rate constant with increasing surface area which was expected since, as mentioned in Section 5.3, there is an increasing reaction rate with surface area.

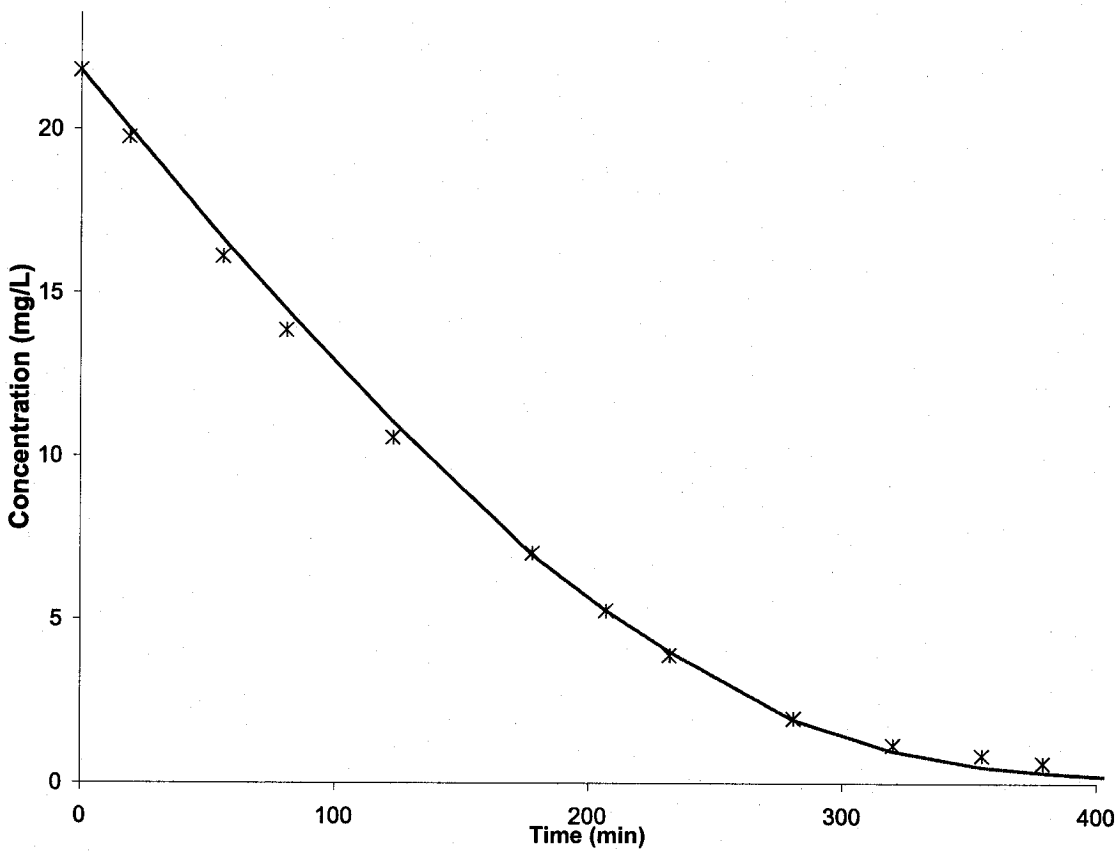

Figure 5.12: L-H kinetics for 16 fin drum at 15 rpm, $k_r = 0.1294$ mg/L/min

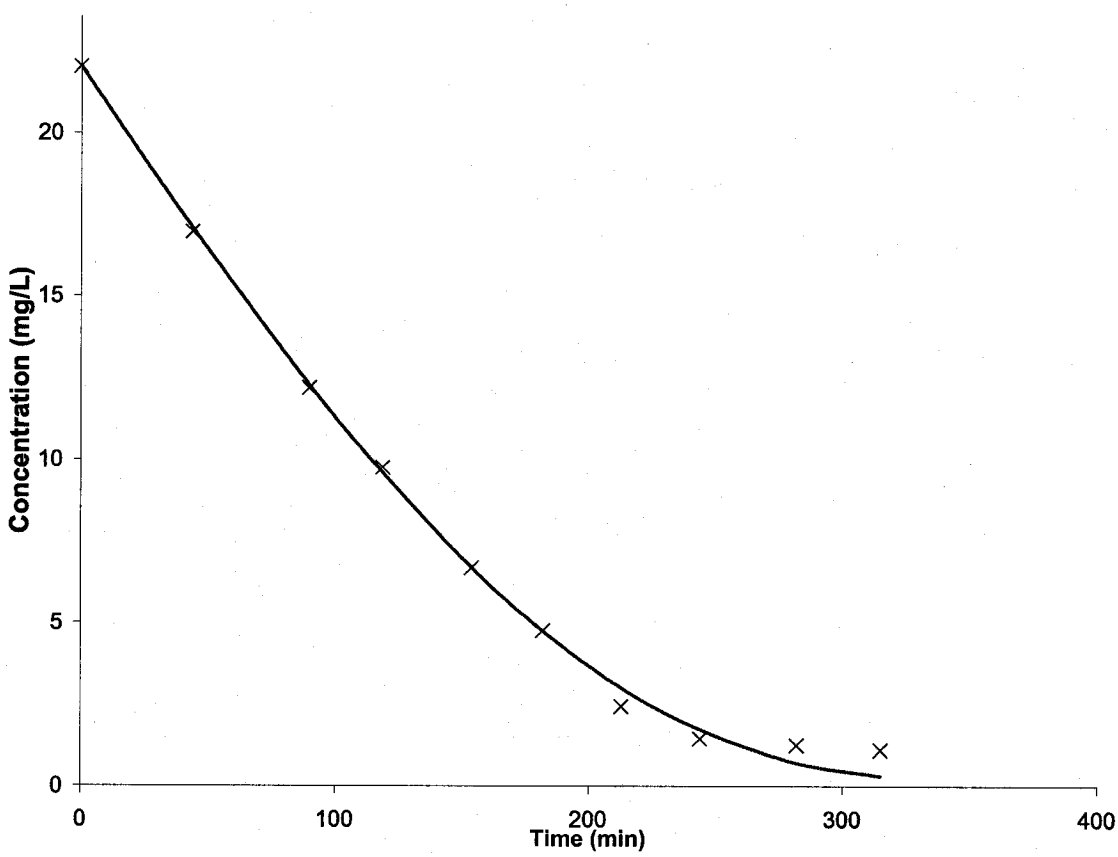

Figure 5.13: L-H kinetics for 40 fin drum at 15 rpm, $k_r = 0.1551$ mg/L/min

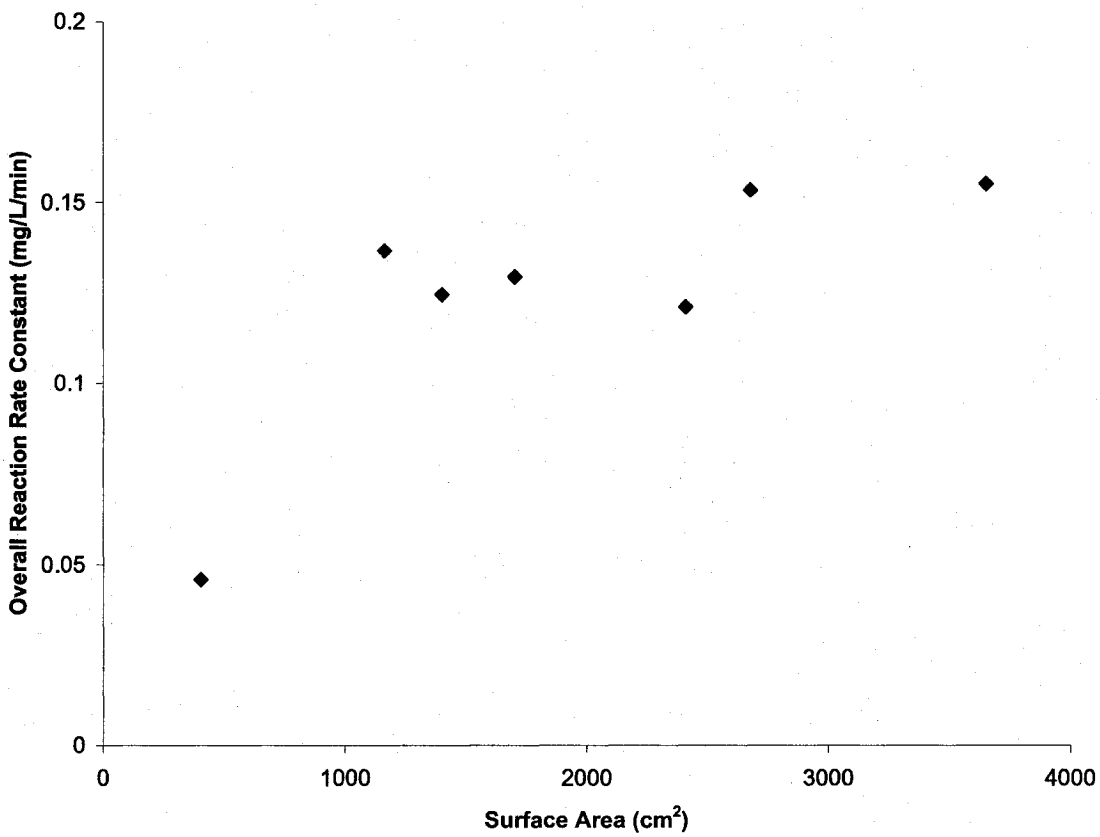

Figure 5.14: L-H overall reaction rate constants at 15 rpm

Chapter 6

Conclusions

This photoreactor demonstrated promising results for the photodegradation of a phenol pollutant in wastewater. The drum configuration design increased the catalyst immobilization surface area and promoted reactant loading at the reaction sites; and the rotation improved agitation, allowed reactant transfer to the illuminated drum surface and exploited periodic illumination effects. From this series of experiments, the photocatalytic reactor design has promising potential for solar-activated wastewater treatment with low manufacturing and operating costs. The following conclusions were drawn from the experimental studies:

- The addition of corrugations significantly improved the performance of the reactor up to 200 %, but it decreased the efficient use of the surface area up to 65 % by decreasing the effective illumination intensity.

- Although increasing the rotational speed did increase the reactant contact with the catalyst, no significant improvement in the reactor performance could be attributed to the rotational speed for the 20 ppm or 40 ppm initial phenol concentration experiments.

- At 5 ppm there was a 76 % increase in the reaction rate between the 15 rpm and 30 rpm experiments indicating a degradation rate limitation based on the ability to deliver reactants to the catalyst surface.

- Between 5 ppm and 20 ppm there was a significant increase in degradation rate with initial concentration, but not between the higher concentrations of 20 ppm and 40 ppm which is consistent with the Langmuir-Hinshelwood reaction kinetics.

- An increase in light intensity increased the degradation rate by 73 % from a single lamp configuration to a three lamp configuration due to the enhanced activation of the catalyst.

- Consideration of the other compounds (besides phenol) present in the reaction medium showed that there were three main reaction intermediates in the system with retention times of 2.98 minutes, 3.20 minutes and 3.98 minutes.

- Langmuir-Hinshelwood kinetics was found to be applicable for this reactor design and the overall reaction rate constant was found to increase with increasing surface area from 0.0458 mg/L/min to 0.1551 mg/L/min. The average adsorption coefficient for phenol in this system was 0.120 L/mg.

Therefore, although very encouraging results were found from this series of experiments, further study is necessary to fully define the potential for this reactor design in industrial settings.

Chapter 7

Recommendations

Based on the results and conclusions from this study on the photocatalytic degradation of phenol, the following recommendations are proposed for future studies to promote the commercialization of photocatalytic wastewater treatment by implementing practical reactor designs.

- A study of titanium dioxide application techniques that accommodate consistent and precise catalyst coating.
- An experimental study of photocatalytic degradation of other compounds under varying operating conditions.
- A study of the treatment of wastewater with varying characteristics and pollutants to provide insight on the practical applications of this photoreactor system and its versatility.
- An experimental optimization of other reaction parameters such as temperature, pH, catalyst loading and dissolved oxygen content to determine the optimal operating conditions for this system.

- Studies of reaction intermediate identification, water film pollutant degradation and residual absorbance correlations for the system.
- Comprehensive modeling to fully describe the kinetics of the photocatalytic degradation.
- An exhaustive study of scaling of this photocatalytic reactor design and the applicability of solar-activated applications.

Execution of these studies will provide well-needed insight as to the practicality of commercial photocatalytic water purification and wastewater treatment facilities.

Appendix A

Spectrophotometer Calibration

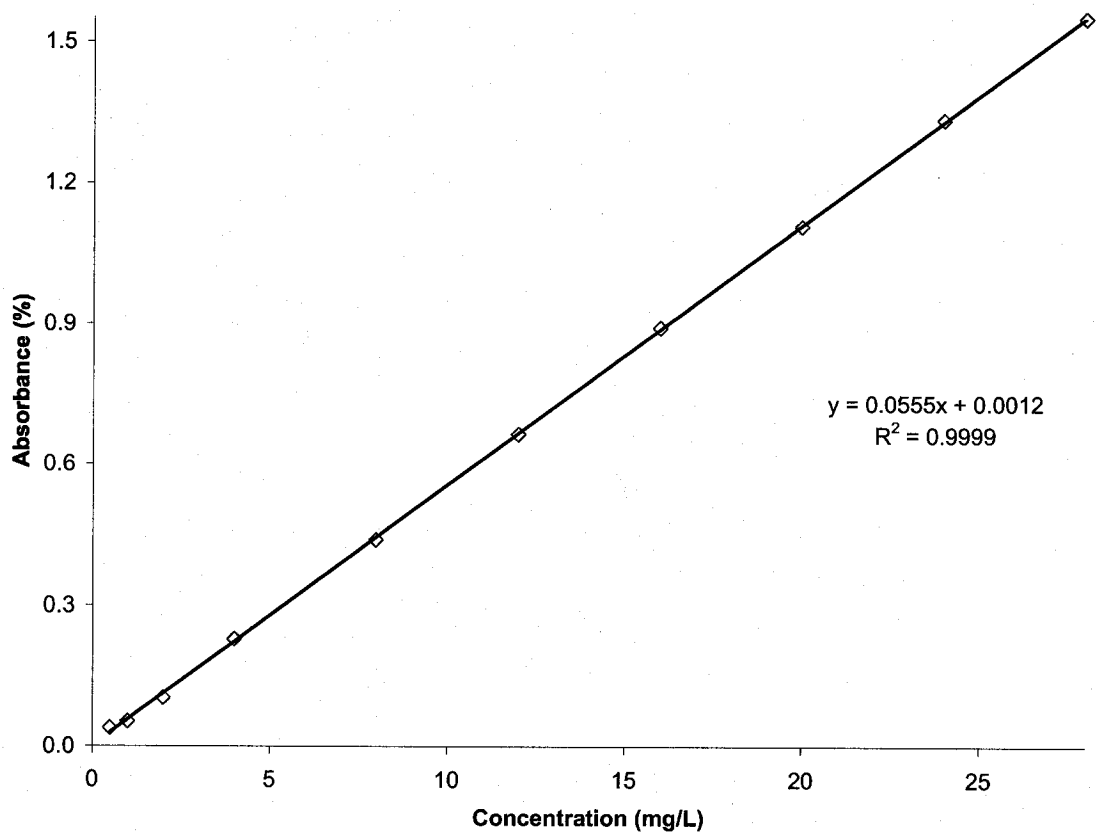

Figure A.1: Spectrophotometer calibration curve for phenol

Appendix B

HPLC Calibration

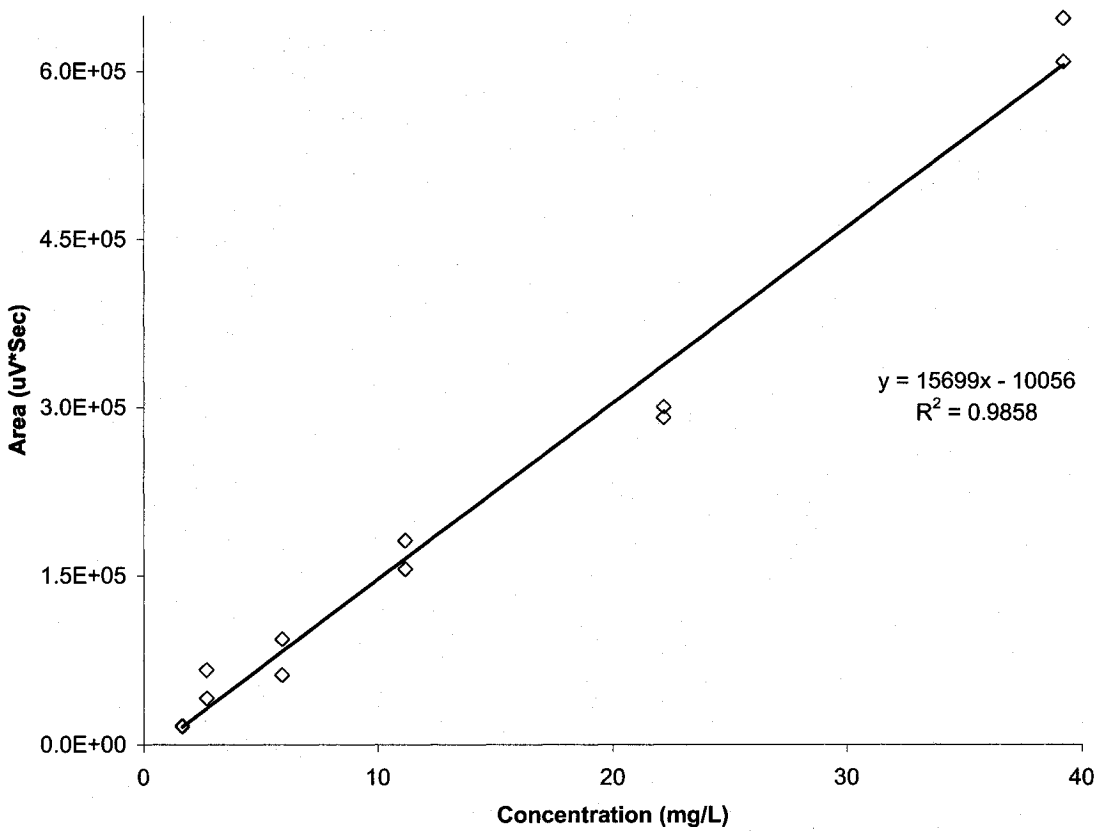

Figure B.1: HPLC calibration curve for phenol

Appendix C

Langmuir-Hinshelwood Kinetics

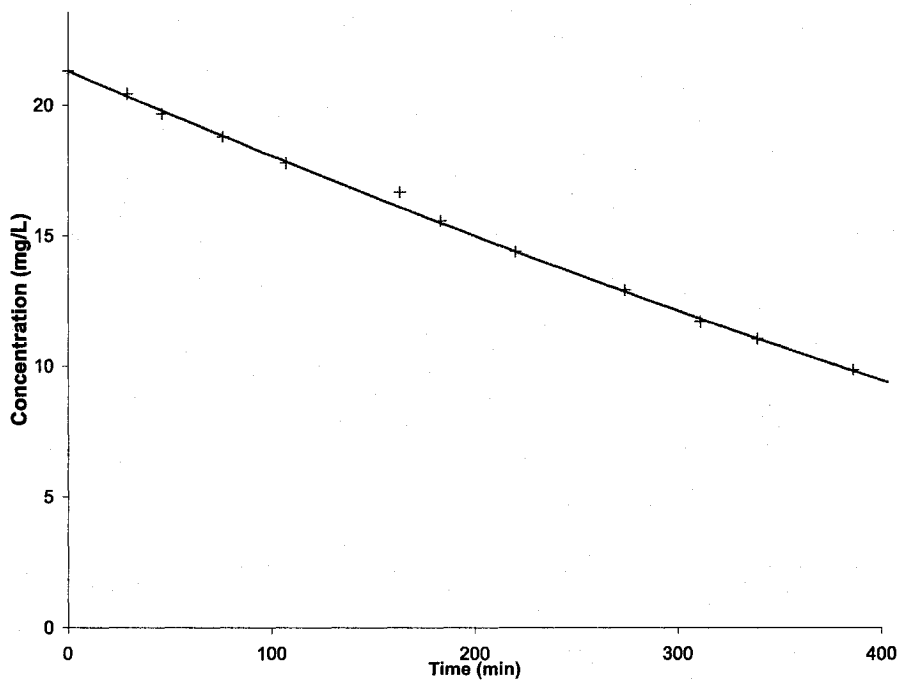

Figure C.1: L-H kinetics: no corrugations $k_r = 0.0458$ mg/L/min

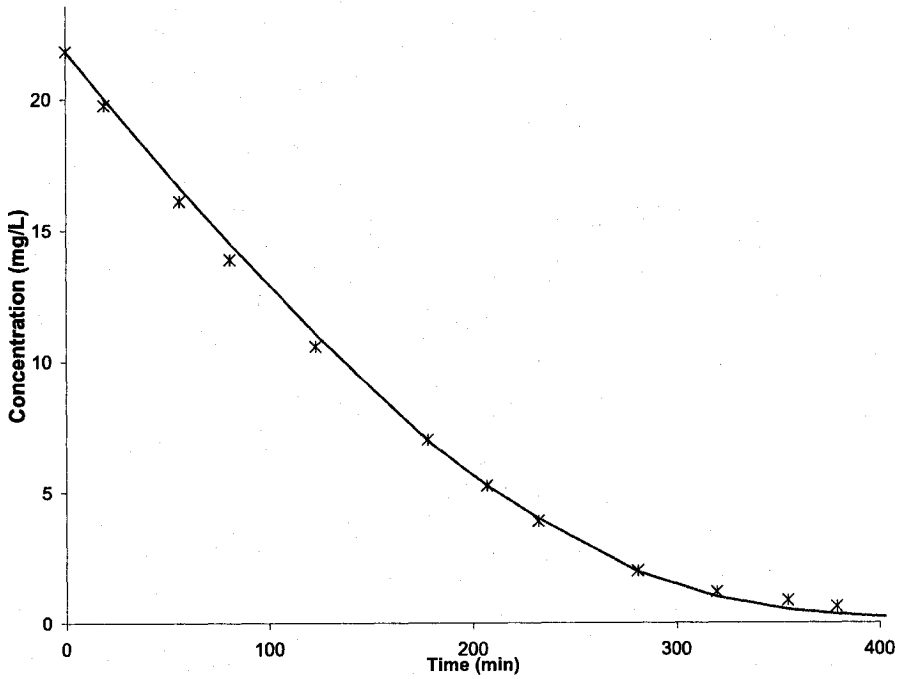

Figure C.2: L-H kinetics: 16 fins $k_r = 0.1294$ mg/L/min

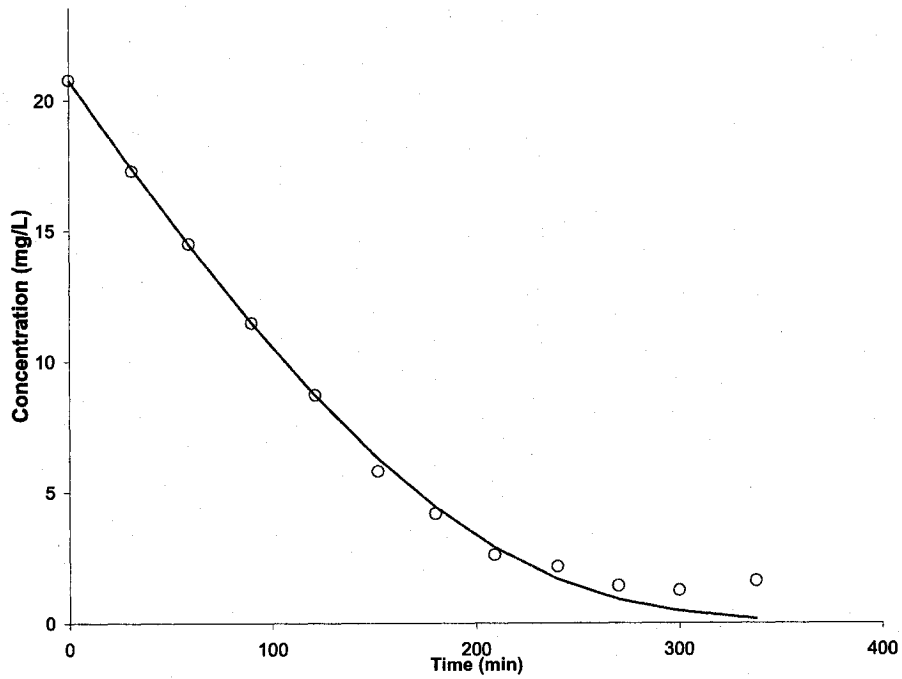

Figure C.3: L-H kinetics: 28 fins $k_r = 0.1534$ mg/L/min

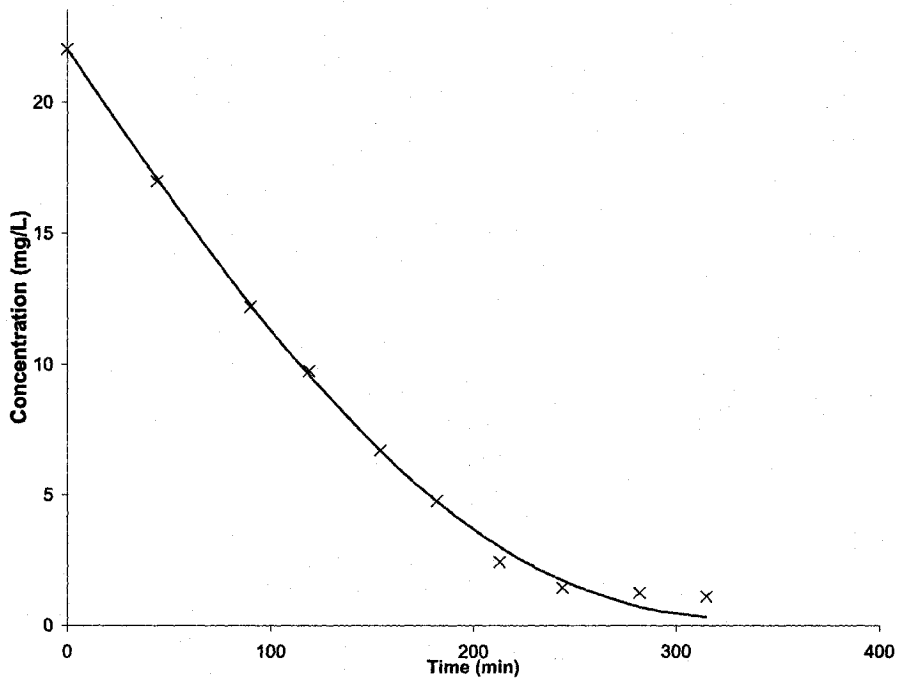

Figure C.4: L-H kinetics: 40 fins $k_r = 0.1551$ mg/L/min

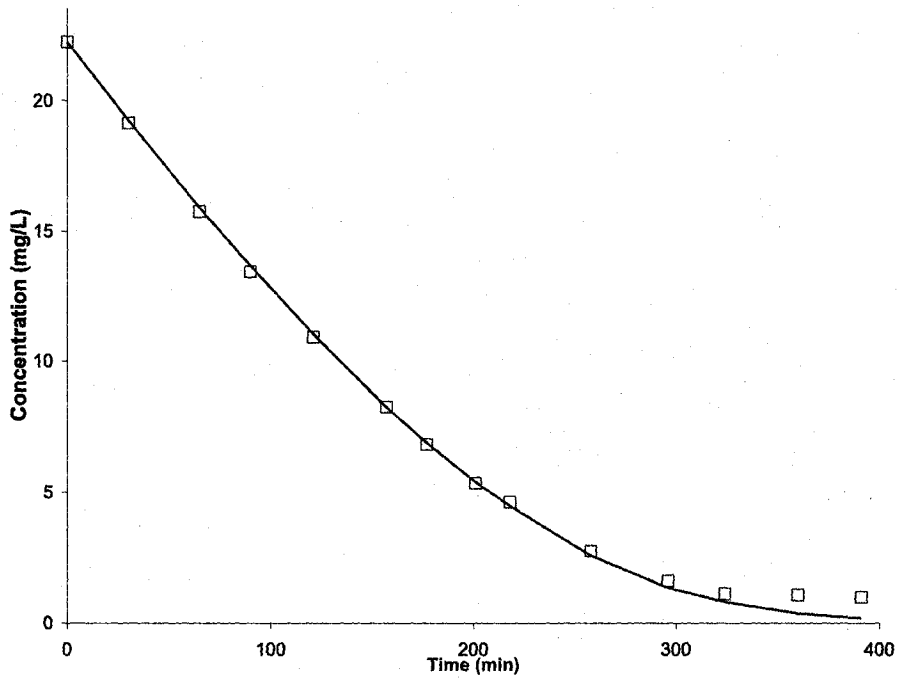

Figure C.5: L-H kinetics: 30° angle $k_r = 0.1366$ mg/L/min

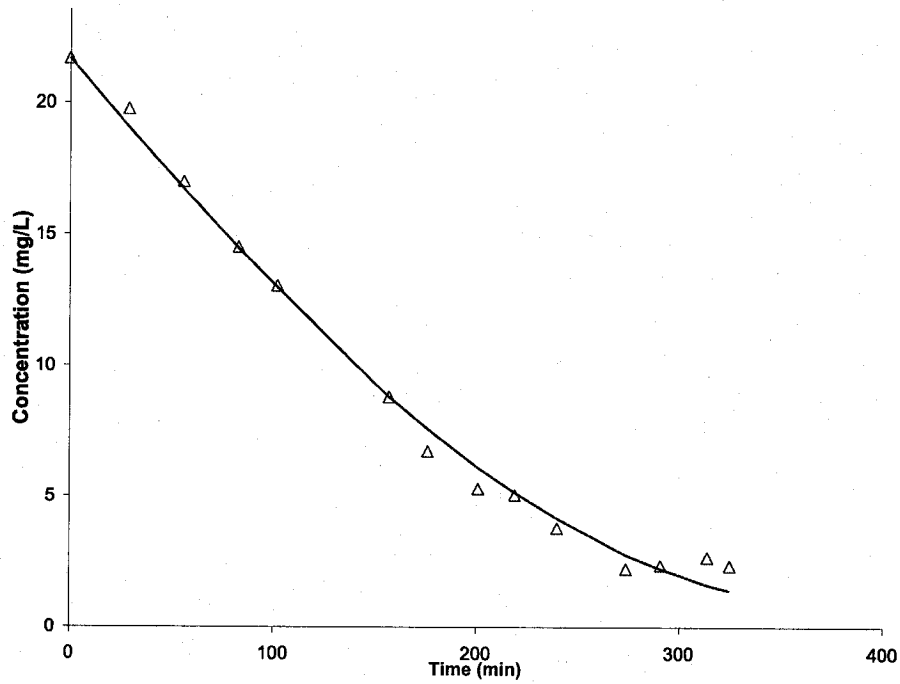

Figure C.6: L-H kinetics: 20° angle $k_r = 0.1245$ mg/L/min

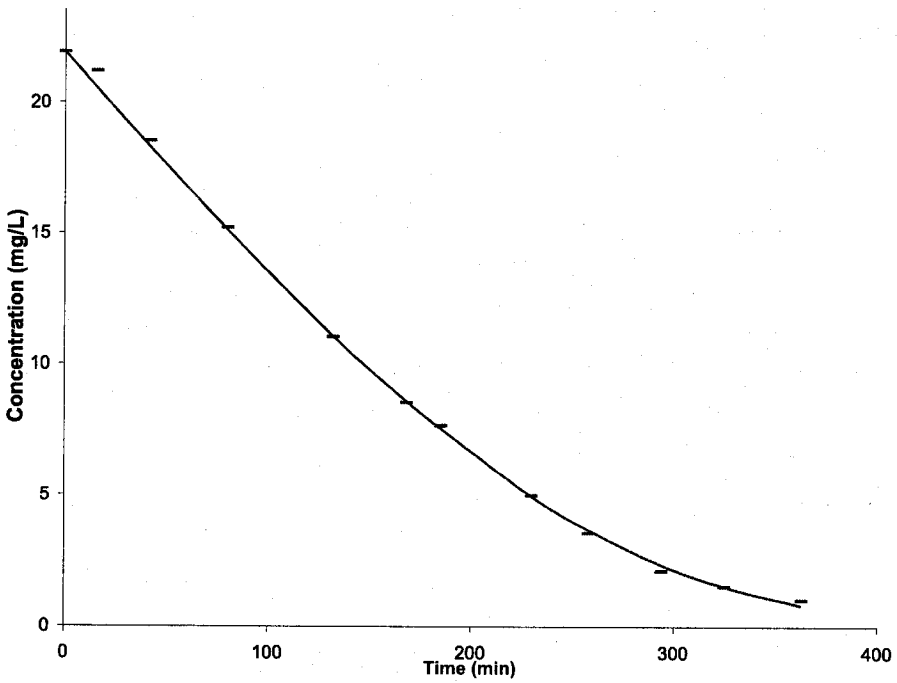

Figure C.7: L-H kinetics: 10° angle $k_r = 0.1211$ mg/L/min

Bibliography

[1] M. Abdullah, G. K.-C. Low, and R. W. Matthews. Effects of common inorganic anions on rates of photocatalytic oxidation of organic carbon over illuminated titanium dioxide. *J. Phys. Chem.*, 94(17):6820–6825, 1990.

[2] A. G. Agrios and P. Pichat. State of the art and perspectives on materials and applications of photocatalysis over TiO_2. *J. Appl. Electrochem.*, 35(7):655–663, 2005.

[3] H. Al-Ekabi and N. Serpone. Kinetic studies in heterogeneous photocatalysis. 1. Photocatalytic degradation of chlorinated phenols in aerated aqueous solutions over TiO_2 supported on a glass matrix. *J. Phys. Chem.*, 92(20):5726–5731, 1988.

[4] H. Al-Ekabi, N. Serpone, E. Pelizzette, C. Minero, M. A. Fox, and R. B. Draper. Kinetic studies in heterogeneous photocatalysis. 2. TiO_2-mediated degradation of 4-chlorophenol alone and in a three-component mixture of 4-chlorophenol, 2,4-dichlorophenol, and 2,4,5-trichlorophenol in air-equilibrated aqueous media. *Langmuir*, 5(1):250–255, 1989.

[5] T.-C. An, Gu. Li, X. Zhu, J. Fu, G. Sheng, and Z. Kun. Photoelectrocatalytic degradation of oxalic acid in aqueous phase with a novel three-dimensional electrode-

hollow quartz tube photoelectrocatalytic reactor. *Appl. Catal., A*, 279(1-2):247–256, 2005.

[6] T.-C. An, M. Zhang, X. Wang, G. Sheng, and J. Fu. Photocatalytic degradation of gaseous trichloroethene using immobilized ZnO/SnO_2 coupled oxide in a flow-through photocatalytic reactor. *J. Chem. Technol. Biotechnol.*, 80(3):251, 2005.

[7] T.-C. An, X.-H. Zhu, and Y. Xiong. Feasibility study of photoelectrochemical degradation of methylene blue with three-dimensional electrode-photocatalytic reactor. *Chemosphere*, 46(6):897–903, 2002.

[8] R. Andreozzi, V. Caprio, A. Insola, G. Longo, and V. Tufano. Photocatalytic oxidation of 4-nitrophenol in aqueous TiO_2 slurries: An experimental validation of literature kinetic models. *J. Chem. Technol. Biotechnol.*, 75(2):131–136, 2000.

[9] A.-K. Axelsson and L. J. Dunne. Mechanism of photocatalytic oxidation of 3,4-dichlorophenol on TiO_2 semiconductor surfaces. *J. Photochem. Photobiol., A*, 144(2-3):205–213, 2001.

[10] D. Bahnemann. Photocatalytic water treatment: Solar energy applications. *Sol. Energy*, 77(5):445–459, 2004.

[11] D. S. Bhatkhande, V. G. Pangarkar, and A. A. C. M. Beenackers. Photocatalytic degradation for environmental applications — A review. *J. Chem. Technol. Biotechnol.*, 77(1):102–116, 2001.

[12] D. Chen and A. K. Ray. Photodegradation kinetics of 4-nitrophenol in TiO_2 suspension. *Water Res.*, 32(11):3223–3234, 1998.

[13] D. H. Chen, X. Ye, and K. Li. Oxidation of PCE with a UV LED photocatalytic reactor. *Chem. Eng. Technol.*, 28(1):95, 2005.

[14] W.-M. Chen, J.-S. Chang, C.-H. Wu, and S.-C. Chang. Characterization of phenol and trichloroethene degradation by the rhizobium Ralstonia taiwanensis. *Res. Microbiol.*, 155(8):672–680, 2004.

[15] G. Chester, M. Anderson, H. Read, and S. Esplugas. A jacketed annular membrane photocatalytic reactor for wastewater treatment: Degradation of formic acid and atrazine. *J. Photochem. Photobiol., A*, 71(3):291–297, 1993.

[16] J. C. Crittenden, J. Liu, D. W. Hand, and D. L. Perram. Photocatalytic oxidation of chlorinated hydrocarbons in water. *Water Res.*, 31(3):429–438, 1997.

[17] D. D. Dionysiou, G. Balasubramanian, M. T. Suidan, A. P. Khodadoust, Isabelle Baudin, and Jean-Michel Laîné. Rotating disk photocatalytic reactor: Development, characterization, and evaluation for the destruction of organic pollutants in water. *Water Res.*, 34(11):2927–2940, 2000.

[18] D. D. Dionysiou, A. P. Khodadoust, A. M. Kern, M. T. Suidan, I. Baudin, and J.-M. Laîné. Continuous-mode photocatalytic degradation of chlorinated phenols and pesticides in water using a bench-scale TiO_2 rotating disk reactor. *Appl. Catal., B*, 24(3-4):139–155, 2000.

[19] D. D. Dionysiou, M. T. Suidan, I. Baudin, and J.-M. Laîné. Oxidation of organic contaminants in a rotating disk photocatalytic reactor: Reaction kinetics in the liquid phase and the role of mass. *Appl. Catal., B*, 38(1):1–16, 2002.

[20] S. J. B. Duff, K. J. Kennedy, and A. J. Brady. Treatment of dilute phenol/PCP wastewaters using the upflow anaerobic sludge blanket (USAB) reactor. *Water Res.*, 29(2):645–651, 1995.

[21] P. K. Dutta and A. K. Ray. Experimental investigation of Taylor vortex photocatalytic reactor for water purification. *Chem. Eng. Sci.*, 59(22-23):5249–5259, 2004.

[22] K. K. Ermolaev and O. G. Mironov. The role of phenol destroying microorganisms in the process of phenol degradation in the Black Sea. *Mikrobiologiya*, 44(5):928–932, 1975.

[23] A. J. Feitz, B. H. Boyden, and T. D. Waite. Evaluation of two solar pilot scale fixed-bed photocatalytic reactors. *Water Res.*, 34(16):3927–3932, 2000.

[24] M. A. Fox and M. T. Dulay. Heterogeneous photocatalysis. *Chem. Rev.*, 93(1):341–357, 1993.

[25] S. Goldstein, G. Czapski, and J. Rabani. Oxidation of phenol by radiolytically generated $\cdot OH$ and chemically generated $SO_4\cdot$. A distinction between $\cdot OH$ transfer and hole oxidation in the photolysis of TiO_2 colloid solution. *J. Phys. Chem.*, 98(26):6586–6591, 1994.

[26] M. M. Halmann. *Photodegradation of Water Pollutants.* CRC Press, Inc., New York, United States of America, 1996.

[27] N. A. Hamill, L. R. Weatherley, and C. Hardacre. Use of a batch rotating photocatalytic contactor for the degradation of organic pollutants in wastewater. *Appl. Catal., B*, 30(1-2):49–60, 2001.

[28] J.-M. Herrmann. Heterogeneous photocatalysis: State of the art and present applications. *Top. Catal.*, 34(1-4):49–65, 2005.

[29] M. R. Hoffmann, S. T. Martin, W. Choi, and D. W. Bahnemann. Environmental applications of semiconductor photocatalysis. *Chem. Rev.*, 95(1):69–96, 1995.

[30] K. Hofstadler and R. Bauer. New reactor design for photocatalytic wastewater treatment with TiO_2 immobilized on fused-silica glass fibers: Photomineralization of 4-chlorophenol. *Environ. Sci. Technol.*, 28(4):670–674, 1994.

[31] Fraunhofer Institut für Silicatforschung ISC. Development of a novel reactor type for waste water treatment based on photocatalysis. `www.isc.fraunhofer.de`, June 2006.

[32] H. S. Joglekar, S. D. Samant, and J. B. Joshi. Kinetics of wet air oxidation of phenol and substituted phenols. *Water Res.*, 25(2):135–145, 1991.

[33] M. Kaneko and I. Okura. *Photocatalysis: Science and Technology.* Biological and Medical Physics Ser. Springer, 2003.

[34] J. K. Kim, H. S. Choi, E. Kim, Y. S. Lee, Y. H. Kim, and S. W. Kim. Comparative effects of TiO_2-immobilized photocatalytic supporters on the bactericidal efficiency of a novel photoreactor. *Biotechnol. Lett.*, 24(17):1397–1400, 2002.

[35] K.-W. Kim, E.-H. Lee, Y.-J. Kim, M.-H. Lee, and D.-W. Shin. A study on characteristics of an electrolytic-photocatalytic reactor using an anode coated with TiO_2. *J. Photochem. Photobiol., A*, 161(1):11–20, 2003.

[36] L. M. Kondrat'eva, E. A. Karetnikova, and V. L. Rapoport. Degradation of phenol compounds by microbial communities of the Amur estuary. *Russ. J. Mar. Biol./Biol. Morya*, 27(6):353, 2001.

[37] Y. Ku and C.-B. Hsieh. Photocatalytic decomposition of 2,4-dichlorophenol in aqueous TiO_2 suspensions. *Water Res.*, 26(11):1451–1456, 1992.

[38] S. A. Kumar and S. Kanmani. Solar photocatalytic degradation of phenolic wastewaters: Investigation of the effect of operational parameters. *Indian J. Environ. Prot.*, 25(1):51–56, 2005.

[39] X. Z. Li and Y. G. Zhao. On-site treatment of dyeing wastewater by a bio-photoreactor system. *Water Sci. Technol.*, 36(2-3):165–172, 1997.

[40] X. Z. Li and Y. G. Zhao. Advanced treatment of dyeing wastewater for reuse. *Water Sci. Technol.*, 39(10-11):249–255, 1999.

[41] H. F. Lin and K. T. Valsaraj. Development of an optical fiber monolith reactor for photocatalytic wastewater treatment. *J. Appl. Electrochem.*, 35(7):699–708, 2005.

[42] C. M. Ling, A. R. Mohamed, and S. Bhatia. Performance of photocatalytic reactors using immobilized TiO_2 film for the degradation of phenol and methylene blue dye present in water stream. *Chemosphere*, 57(7):547–554, 2004.

[43] I. N. Martyanov, E. N. Savinov, and V. N. Parmon. A comparative study of efficiency of photooxidation of organic contaminants in water solutions in various photochemical and photocatalytic systems: 1. Phenol photooxidation promoted by hydrogen peroxide in a flow reactor. *J. Photochem. Photobiol., A*, 107(1-3):227–231, 1997.

[44] R. W. Matthews and S. R. McEvoy. A comparison of 254 nm and 350 nm excitation of TiO_2 in simple photocatalytic reactors. *J. Photochem. Photobiol., A*, 66(3):355–366, 1992.

[45] R. W. Matthews and S. R. McEvoy. Photocatalytic degradation of phenol in the presence of near-UV illuminated titanium dioxide. *J. Photochem. Photobiol., A*, 64:231–246, 1992.

[46] M. Mehrvar, W. A. Anderson, and M. Moo-Young. Preliminary analysis of a tellerette packed-bed photocatalytic reactor. *Adv. Chem. Res.*, 6(4):411–418, 2002.

[47] B. V. Mihaylov, J. L. Hendrix, and J. H. Nelson. Comparative catalytic activity of selected metal oxides and sulfides for the photo-oxidation of cyanide. *J. Photochem. Photobiol., A*, 72(2):173–177, 1993.

[48] A. Moharikar and H. J. Purohit. Specific ratio and survival of Pseudomonas CF600 as co-culture for phenol degradation in continuous cultivation. *Int. Biodeterior. Biodegrad.*, 52(4):255–260, 2003.

[49] G. Neumann, R. Teras, L. Monson, M. Kivisaar, F. Schauer, and H. J. Heipieper. Simultaneous degradation of atrazine and phenol by Pseudomonas sp. strain ADP: Effects of toxicity and adaptation. *Appl. Environ. Microbiol.*, 70(4):1907–1912, 2004.

[50] Y. M. Nor. Phenol removal by Eichhornia crassipes in the presence of trace metals. *Water Res.*, 28(5):1161–1166, 1994.

[51] D. F. Ollis, E. Pelizzetti, and N. Serpone. Destruction of water contaminants. *Environ. Sci. Technol.*, 25(9):1523–1529, 1991.

[52] T. Oppenländer. *Photochemical Purification of Water and Air: Advanced Oxidation Processes (AOPs) : Principles, Reaction Mechanisms, Reactor Concepts.* John Wiley & Sons, Incorporated, United States, 2003.

[53] Y. Parent, D. Blake, K. Magrini-Bair, C. Lyons, C. Turchi, A. Watt, E. Wolfrum, and M. Prairie. Solar photocatalytic processes for the purification of water: State of development and barriers to commercialization. *Sol. Energy*, 56(5):429–437, 1996.

[54] S. V. Preis, S. B. Kamenev, and Yul Kallas. Oxidative purification of phenol containing waste water of thermal oil shale treatment. *Khim. Tekhnol. Vody*, 16(1):83–91, 1994.

[55] G. L. Puma and P. L. Yue. A novel fountain photocatalytic reactor for water treatment and purification: Modeling and design. *Ind. Eng. Chem. Res.*, 40(23):5162–5169, 2001.

[56] G. L. Puma and P. L. Yue. A novel fountain photocatalytic reactor: Model development and experimental validation. *Chem. Eng. Sci.*, 56(8):2733–2744, 2001.

[57] Purifics. Photo-Cat® Water. `www.purifics.com`, June 2006.

[58] A. K. Ray. A new photocatalytic reactor for destruction of toxic water pollutants by advanced oxidation process. *Catal. Today*, 44(1-4):357–368, 1998.

[59] A. K. Ray. Design, modelling and experimentation of a new large-scale photocatalytic reactor for water treatment. *Chem. Eng. Sci.*, 54(15-16):3113–3125, 1999.

[60] L. Rideh, A. Wehrer, D. Ronze, and A. Zoulalian. Modelling of the kinetic of 2-chlorophenol catalytic photooxidation. *Catal. Today*, 48(1-4):357–362, 1999.

[61] J. G. Sczechowski, C. A. Koval, and R. D. Noble. Evidence of critical illumination and dark recovery times for increasing the photoefficiency of aqueous heterogeneous photocatalysis. *J. Photochem. Photobiol., A*, 74:273–278, 1993.

[62] J. G. Sczechowski, C. A. Koval, and R. D. Noble. Use of controlled periodic illumination for an improved method of photocatalysis and an improved reactor design. US19930129849 19930930(US5439652), 1995.

[63] T. K. Sengupta, M. F. Kabir, and A. K. Ray. A Taylor vortex photocatalytic reactor for water purification. *Ind. Eng. Chem. Res.*, 40(23):5268–5281, 2001.

[64] B. Serrano and H. de Lasa. Photocatalytic degradation of water organic pollutants: Pollutant reactivity and kinetic modeling. *Chem. Eng. Sci.*, 54(15-16):3063–3069, 1999.

[65] H. Shang, Z. Zhang, and W. A. Anderson. Nonuniform radiation modeling of a corrugated plate photocatalytic reactor. *AIChE J.*, 51(7):2024–2033, 2005.

[66] S. Shashirekha, L. Uma, and G. Subramanian. Phenol degradation by the marine cyanobacterium Phormidium valderianum BDU 30501. *J. Ind. Microbiol. Biotechnol.*, 19(2):130–133, 1997.

[67] G. S. Shephard, S. Stockenström, D. de Villiers, W. J. Engelbrecht, and G. F. S. Wessels. Degradation of microcystin toxins in a falling film photocatalytic reactor with immobilized titanium dioxide catalyst. *Water Res.*, 36(1):140–146, 2002.

[68] Y. Shinoda, Y. Sakai, M. Ue, A. Hiraishi, and N. Kato. Isolation and characterization of a new denitrifying spirillum capable of anaerobic degradation of phenol. *Appl. Environ. Microbiol.*, 66(4):1286–1291, 2000.

[69] F. Shiraishi, K. Fukinbara Toyoda S., E. Obuchi, and K. Nakano. Photolytic and photocatalytic treatment of an aqueous solution containing microbial cells and organic compounds in an annular-flow reactor. *Chem. Eng. Sci.*, 54(10):1547–1552, 1999.

[70] A. Sobczyński, L. Duczmal, and W. Zmudzinski. Phenol destruction by photocatalysis on TiO_2: An attempt to solve the reaction mechanism. *J. Mol. Catal. A: Chem.*, 213(2):225–230, 2004.

[71] S. Tanaka and U. K. Saha. Effects of pH on photocatalysis of 2,4,6-trichlorophenol in aqueous TiO_2 suspensions. *Water Sci. Technol.*, 30(9):47–57, 1994.

[72] J. Theurich, M. Lindner, and D. W. Bahnemann. Photocatalytic degradation of 4-chlorophenol in aerated aqueous titanium dioxide suspensions: A kinetic and mechanistic study. *Langmuir*, 12(26):6368–6376, 1996.

[73] H. B. Thu, M. Karkmaz, E. Puzenat, C. Guillard, and J. M Herrmann. From the fundamentals of photocatalysis to its applications in environment protection and in solar purification of water in arid countries. *Res. Chem. Intermed.*, 31(4-6):449–461, 2005.

[74] M. Trillas, J. Peral, and X. Domeñech. Photo-oxidation of phenoxyacetic acid by TiO_2-illuminated catalyst. *Appl. Catal., B*, 3(1):45–53, 1993.

[75] M. Trillas, J. Peral, and X. Domeñech. Photocatalyzed degradation of phenol, 2,4-dichlorophenol, phenoxyacetic acid and 2,4-dichlorophenoxyacetic acid over supported TiO_2 in a flow system. *J. Chem. Technol. Biotechnol.*, 67(3):237–242, 1996.

[76] C. S. Turchi and D. F. Ollis. Mixed reactant photocatalysis: Intermediates and mutual rate inhibition. *J. Catal.*, 119(2):483–496, 1989.

[77] E. Vaisman, M. F. Kabir, A. Kantzas, and C. H. Langford. A fluidized bed photoreactor exploiting a supported photocatalyst with adsorption pre-concentration capacity. *J. Appl. Electrochem.*, 35(7):675–681, 2005.

[78] R. Villacres, S. Ikeda, T. Torimoto, and B. Ohtani. Development of a novel photocatalytic reaction system for oxidative decomposition of volatile organic compounds in water with enhanced aeration. *J. Photochem. Photobiol., A*, 160(1-2):121–126, 2003.

[79] M. Wurster, S. Mundt, E. Hammer, F. Schauer, and U. Lindequist. Extracellular degradation of phenol by the cyanobacterium Synechococcus PCC 7002. *J. Appl. Phycol.*, 15(2-3):171–176, 2003.

[80] H. C. Yatmaz, C. Wallis, and C. R. Howarth. The spinning disc reactor — Studies on a novel TiO_2 photocatalytic reactor. *Chemosphere*, 42(4):397–403, 2001.

[81] A. A. Yawalkar, D. S. Bhatkhande, V. G. Pangarkar, and A. A. C. M. Beenackers. Solar-assisted photochemical and photocatalytic degradation of phenol. *J. Chem. Technol. Biotechnol.*, 76(4):363, 2001.

[82] H. Zhang, H. Luo, and Y. Kamagata. Characterization of the phenol hydroxylase from Burkholderia kururiensis KP23 involved in trichloroethylene degradation by gene cloning and disruption. *Microbes Environ.*, 18(3):167–173, 2003.

[83] L. Zhang, T. Kanki, N. Sano, and A. Toyoda. Photocatalytic degradation of organic compounds in aqueous solution by a TiO_2-coated rotating-drum reactor using solar light. *Sol. Energy*, 70(4):331–337, 2001.

[84] L. Zhang, T. Kanki, N. Sano, and A. Toyoda. Development of TiO_2 photocatalyst reaction for water purification. *Sep. Purif. Technol.*, 31(1):105, 2003.

[85] Z. Zhang, W. A. Anderson, and M. Moo-Young. Rigorous modeling of UV absorption by TiO_2 films in a photocatalytic reactor. *AIChE J.*, 46(7):1461–1467, 2000.

[86] Z. Zhang, W. A. Anderson, and M. Moo-Young. Photocatalytic pretreatment of contaminated groundwater for biological nitrification enhancement. *J. Chem. Technol. Biotechnol.*, 77(2):190, 2002.

[87] Z. Zhang, W. A. Anderson, and M. Moo-Young. Modeling of corrugated plate photocatalytic reactors and experimental validation. *Chem. Eng. Sci.*, 58(3-6):911–914, 2003.

[88] Z. Zhang, W. A. Anderson, and M. Moo-Young. Experimental analysis of a corrugated plate photocatalytic reactor. *Chem. Eng. J.*, 99(2):145–152, 2004.